Exploring the genetic and functional diversity of *Porphyromonas gingivalis* long fimbriae

Von der Medizinischen Fakultät
der Rheinisch-Westfälischen Technischen Hochschule Aachen
zur Erlangung des akademischen Grades eines Doktors der Zahnmedizin
genehmigte Dissertation

vorgelegt von

Hendrik Leonhard Meyer

aus Hamburg

Berichter: Univ.-Prof. Dr. rer. nat. Georg Conrads
Priv.-Doz. Dr. rer. nat. Mark van der Linden

Tag der mündlichen Prüfung: 13.06.2024

Diese Dissertation ist auf den Internetseiten der Universitätsbibliothek online verfügbar.

Die Publikation, die die Dissertation darstellt:

Meyer, Hendrik Leonhard, Abdelbary, Mohamed M. H., Buhl, Eva Miriam, Kuppe, Christoph, Conrads, Georg

Exploring the genetic and functional diversity of *Porphyromonas gingivalis* long fimbriae

Molecular Oral Microbiology, 38: 408-423, 2023

D 82 (Diss. RWTH Aachen University, 2024)

Check for updates

Received: 14 June 2023 | Revised: 8 August 2023 | Accepted: 11 September 2023

DOI: 10.1111/omi.12433

ORIGINAL ARTICLE

WILEY

Exploring the genetic and functional diversity of *Porphyromonas gingivalis* long fimbriae

Hendrik Leonhard Meyer[1] | Mohamed M. H. Abdelbary[1] | Eva Miriam Buhl[2] | Christoph Kuppe[3] | Georg Conrads[1]

[1]Division of Oral Microbiology and Immunology, Department of Operative Dentistry, Periodontology and Preventive Dentistry, Rheinisch-Westfälische Technische Hochschule University Hospital, Aachen, Germany

[2]Electron Microscopy Facility, Institute of Pathology, Rheinisch-Westfälische Technische Hochschule University Hospital, Aachen, Germany

[3]Institute of Experimental Medicine and Systems Biology, RWTH Aachen University, Aachen, Germany

Correspondence
Georg Conrads, Division of Oral Microbiology and Immunology, Department of Operative Dentistry, Periodontology and Preventive Dentistry, RWTH University of Aachen, Pauwelsstr. 30, 52057 Aachen, Germany.
Email: gconrads@ukaachen.de

Funding information
Interdisciplinary Center for Clinical Research of the RWTH Aachen Medical Faculty, Grant/Award Number: OC1-06; Deutsche Forschungsgemeinschaft (DFG), Grant/Award Number: 495328185

Abstract

Porphyromonas gingivalis is a key pathobiont in periodontitis. Its long fimbriae consist of a single anchor (FimB), a varying number of stalk (FimA), and three accessory (tip-related) proteins (FimC, FimD, and FimE). Based on 133 strains/genomes available, it was our aim to investigate the diversity within FimA and FimB and explain the variety of long fimbriae (super-)structures. Combining the new forward primer fimAnewF with the established fimAunivR, we were able to amplify and sequence *fimA* including its leader region covering all genotypes and serotypes for phylogenetic analysis. We designed two primer pairs sensing the presence of an internal stop codon in *fimB* with an impact on fimbrial length. Finally, we examined fimbrial secondary structures by transmission electron microscopy (TEM) and scanning electron microscopy (SEM). The phylogeny of *fimA*/FimA revealed two new subtypes (IIa and IIb) with specific changes in functional domains and thus adding to the current classification scheme (I, Ib, and II-V). Regarding evolution, we confirm that *Porphyromonas gulae fimA*-type A is closely related to human *P. gingivalis* strains of cluster Ib and might be its ancestor genotype. A *fimB* internal stop codon is rare and was found in ATCC 33277 only. Comparing *P. gingivalis* TEM/SEM pictures of type I ATCC 33277 with type V OMI622 revealed a broad spectrum of fimbrial structures including bundling, cell-cell knotting, and brick-wall formation. In conclusion, FimA forms more distinct subtypes than previously known. The bundling of long fimbriae, a mechanism known from EPEC/EHEC and *Salmonella*, is proposed and supported by TEM/SEM pictures for the first time here. The role and variations of terminal accessory FimC-E in superstructure formation and/or (co-) adhesion should be investigated more closely next.

KEYWORDS
FimA serotypes, *fimAB* genotypes, long fimbriae, periodontitis, phylogeny, *Porphyromonas gingivalis*, TEM and SEM

Abbreviations: NCBI, National Center for Biotechnology Information; SEM, scanning electron microscopy; TEM, transmission electron microscopy; TSBA, tryptone soya blood agar.

This is an open access article under the terms of the Creative Commons Attribution-NonCommercial-NoDerivs License, which permits use and distribution in any medium, provided the original work is properly cited, the use is non-commercial and no modifications or adaptations are made.
© 2023 The Authors. *Molecular Oral Microbiology* published by John Wiley & Sons Ltd.

1 | INTRODUCTION

Periodontitis is a bacterial infection of the periodontium that leads to varying degrees of tissue loss around the teeth and jawbone resorption. It is one of the major causes of tooth loss today and is one of the most prevalent diseases worldwide (Kassebaum et al., 2017). Severe periodontitis affected 1.1 billion people in 2019, and the prevalence of the disease increased by 8.44% between 1990 and 2019 (M. X. Chen et al., 2021), mainly due to an aging population in industrialized countries. Periodontitis results from a complex interaction of various factors. Primarily, the change from a physiological to a pathogenic biofilm drives an inflammatory response, leading to bone and connective tissue destruction. In addition, the presence of other risk factors such as smoking, a genetic disposition, systematic diseases, or psychological stress is supportive for the development of periodontitis (Tatakis & Kumar, 2005). *Porphyromonas gingivalis* is known as a keystone pathogen and a representative of the so-called red complex of periodontopathic bacteria. A keystone pathogen is characterized by its ability to transform a benign microbiome into a dysbiotic one, even though it may be present only in small amounts in the biofilm (Hajishengallis et al., 2012). As such a "master of dysbiosis," *P. gingivalis* may be the most important bacterial species for the development of periodontitis (Tatakis & Kumar, 2005). Increasingly recognized, the oral pathogen is thought to also be involved in non-oral diseases such as coronary artery disease, stroke, diabetes mellitus, preterm birth/low birth weight, lupus erythematosus, rheumatoid arthritis, oral squamous cell carcinoma, and Alzheimer's disease, to name only a few of possible odontogenic sequelae (Q. Chen et al., 2021; Dominy et al., 2019; Joshi et al., 2022; Kebschull et al., 2010; Madianos et al., 2013; Maresz et al., 2013; Martínez et al., 2021; Mercado et al., 2000; Nezu et al., 2022). *Porphyromonas gingivalis* has a number of virulence factors such as fimbriae (pili), lipopolysaccharide, capsule, potent proteases such as Arg- and Lys-gingipains, and hemagglutinins (Holt & Ebersole, 2005). The fimbriae of *P. gingivalis* are lamellar appendages on the cell surface composed of various proteins. Fimbriae play a critical role in biofilm formation, auto- (self-)aggregation, co-aggregation with other bacteria, adhesion to host molecules, and, subsequently, host cell invasion (Enersen et al., 2013; Hamada et al., 1998; Lamont & Yilmaz, 2002; Yoshimura et al., 2009). Furthermore, recent studies demonstrate a direct role of fimbriae in osteoclastogenesis and thus alveolar bone resorption as well as in the activation of the toll-like receptor-2 and TLR4/NF-κB signaling pathway (Cai et al., 2019; Suzuki et al., 2022; Wielento et al., 2022). *Porphyromonas gingivalis* expresses long Fim-fimbriae (0.3-1.6 μ, composed of FimA-E) and short Mfa-fimbriae (0.080-0.120 μ, composed of Mfa1-5) side by side. Recent studies suggest that fimbriae of *P. gingivalis* are assembled by a process called protease-mediated polymerization and are thus classified as type V pili (Shibata et al., 2020), which should not be confused with subtype V. To date, the *fimA* gene has been divided into six geno-subtypes (I, Ib, II, III, IV, and V) based on variations in its nucleotide sequence (Amano et al., 1999; Fujiwara et al., 1993; Nakagawa et al., 2000; Nakagawa et al., 2002), related (but not identical) to serotypes and virulence, the latter of which needs to be further determined and is an important motivation here. However, discrepancies between genotype and serotype and virulence exist, mainly due to the diffuse, multi-site annealing PCR typing primers used leading to a mix/confusion in subtypes (Enersen et al., 2008). Regarding virulence, recent structural analyses have shed light on the functional regions of the fimbrial protein. Some regions interact with immune epitopes (CD14, CD11b/CD18), while others interact with different salivary proteins (statherin, PRP1) or are important for the polymerization of FimA monomers (Shibata et al., 2020).

Based on 133 strains/genomes available, it was our aim to investigate the diversity within FimA and its anchor protein FimB and explain the variety of long fimbriae (super-)structures.

2 | MATERIALS AND METHODS

2.1 | Bacterial strains and growth conditions

A total of 133 *P. gingivalis* isolates were analyzed. Of these, 34 isolates came from our own strain collection. The *fimA* and *fimB* genes of these isolates were amplified and sequenced. The *fimA* sequences of the other 99 isolates (or genomes) were downloaded from GenBank of the National Center for Biotechnology Information (NCBI) and translated in silico into the corresponding amino acid (aa) sequences.

Our 34 sequenced isolates were composed of samples of human and animal origin and were from a variety of countries: Germany (9), Sweden (1), England (1), Japan (1), Indonesia (9), Canada (6), the United States (6), and Kenya (1). Of the nine strains from Germany, six were isolated in Aachen from patients with untreated periodontitis. The clinical parameters of these patients were described by our group before (Abdelbary et al., 2022; Stein et al., 2021). The other three German strains were isolated in Freiburg (Clinic of Dental Preservation and Periodontology, University Hospital, Freiburg, Germany; sent in 1997-1998). The remaining 25 strains were provided to us by Dr. D. Deng, Academic Center for Dentistry Amsterdam, The Netherlands (sent in 2021). Strain designations, IDs, *fimA*/*fimB* type, isolation year, and geographical origin are provided in Table 1. All samples were stored at −70°C in cryotubes. For analysis, the 34 isolates were cultured on tryptone soya blood agar (TSBA) and incubated anaerobically (<1% oxygen, ≥13% CO_2; BD GasPakTM EZ Gas Generating Systems) at 37°C for 4-7 days. Among the 99 publicly available *fimA*/FimA sequences, the serotype references (with serotype and accession numbers given in parentheses) used were as follows: *P. gingivalis* ATCC 33277 (type I; D17795), HG1691 (type Ib; AB058848), HW24D1 (type II; D17797), OMZ314 (type II; D17798), OMZ409 (type II; D17799), TDC285 (type II; AB195793), ATCC 49417 (type II or III depending on the source; D17800), BH6/26 (type III; D17801), W83 (Type IV; AE015924), HG564 (type IV; D17802), and HNA99 (type V; AB795792). The geographical distribution of strains/genomes is summarized in Figure S1.

20411014, 2023, 5, Downloaded from https://onlinelibrary.wiley.com/doi/10.1111/omi.12433 by Cochrane Germany, Wiley Online Library on [04/12/2023]. See the Terms and Conditions (https://onlinelibrary.wiley.com/terms-and-conditions) on Wiley Online Library for rules of use; OA articles are governed by the applicable Creative Commons License

TABLE 1 Overview of the 34[a] *P. gingivalis* isolates from our strain collection.

Strain designation	Original code	Id name species	Id of host	Fimbriae type[b]	Anchor protein[c]	Isolation year[h]	Geographical origin
OMI 1080	G 251	*P. gingivalis animal biotype/P. gulae*	Monkey[d]	A	Yes	1989	USA, Florida (Fournier et al., 2001)
OMI 1081	I 372	*P. gingivalis animal biotype/P. gulae*	Monkey[d]	A	Yes	1989	USA, Florida (Fournier et al., 2001)
OMI 1072	I 433	*P. gingivalis animal biotype/P. gulae*	Monkey[d]	A	Yes	1989	USA, Florida (Fournier et al., 2001)
OMI 1060	OMG 1426	*P. gingivalis animal biotype/P. gulae*	Monkey[d]	A	Yes	1989	USA, Florida (Fournier et al., 2001)
OMI 1128	Chien 5B	*P. gingivalis animal biotype/P. gulae*	Dog	A	Yes	<2000	Canada, Quebec (Fournier et al., 2001)
OMI 1076	Chat 2	*P. gingivalis animal biotype/P. gulae*	Cat	A	Yes	<2000	Canada, Quebec (Fournier et al., 2001)
OMI 1127	84Pg1	*P. gingivalis*	Human	Ib	Yes	2002	Indonesia
OMI 1088	59Pg1	*P. gingivalis*	Human	Ib	Yes	1994	Indonesia
OMI 1132	ATCC33277	*P. gingivalis*	Human	I	No	<1981	USA (Slots-J)
OMI 889	MZ 16	*P. gingivalis*	Human	I	Yes	2022	Germany, Aachen
OMI 619	Fr. 048/11-1	*P. gingivalis*	Human	I	Yes	1997	Germany, Freiburg
OMI 621	Fr. 016/16-1	*P. gingivalis*	Human	I	Yes	1997	Germany, Freiburg
OMI 731	AC 08	*P. gingivalis*	Human	I	Yes	2022	Germany, Aachen
OMI 1151	K1	*P. gingivalis*	Human	IIa	Yes	2021	Germany, Kiel
OMI 1090	HW24D-2	*P. gingivalis*	Human	IIa	Yes	<1993	Canada, Quebec
OMI 883	AC 27	*P. gingivalis*	Human	IIa	Yes	2022	Germany, Aachen
OMI 1110	OMG 406	*P. gingivalis*	Human	IIa	Yes	<1993	Kenya
OMI 1067	210Pg1[e]	*P. gingivalis*	Human	IIa	Yes	1994	Indonesia
OMI 1123	210Pg1[e]	*P. gingivalis*	Human	IIa	Yes	2002	Indonesia
OMI 1046	21Pg1[f]	*P. gingivalis*	Human	IIb	Yes	1994	Indonesia
OMI 1104	21Pg1[f]	*P. gingivalis*	Human	IIb	Yes	2002	Indonesia
OMI 1105	168Pg1	*P. gingivalis*	Human	IIb	Yes	1994	Indonesia
OMI 778	AC 38	*P. gingivalis*	Human	IIb	Yes	2022	Germany, Aachen
OMI 1077	23A4	*P. gingivalis*	Human	II–hybrid	Yes	<1993	Canada, Quebec
OMI 1074	7B5	*P. gingivalis*	Human	III	Yes	<1993	Canada, Quebec
OMI 887	AC 26	*P. gingivalis*	Human	III	Yes	2022	Germany, Aachen
OMI 743	AC 04	*P. gingivalis*	Human	III	Yes	2022	Germany, Aachen
OMI 1071	ATCC49417, RB22D	*P. gingivalis*	Human	III	Yes	<1993	Canada, Quebec
OMI 629	W83	*P. gingivalis*	Human	IV	Yes	1991	Germany, Bonn
OMI 1094	HG 1954	*P. gingivalis*	Human	IV	Yes	Unknown	Sweden
OMI 1049	AJW5 (VAG5)	*P. gingivalis*	Human	IV	Yes	1991	USA, Buffalo
OMI 1079	83Pg1[g]	*P. gingivalis*	Human	IV	Yes	1994	Indonesia
OMI 1101	83Pg1[g]	*P. gingivalis*	Human	IV	Yes	2002	Indonesia
OMI 622	Fr. 025/15-1	*P. gingivalis*	Human	V	Yes	1997	Germany, Freiburg

[a]Isolates from one jaguar (*P. gingivalis/circumdentaria*) and two sheep (*P. gingivalis/loveana*) were additionally examined but could not be amplified.
[b]Based on variations in the nucleotide sequences of *fimA*.
[c]Encoded by *fimB* gene.
[d]From common squirrel monkey.
[e]Strain OMI 1067 and OMI 1123 were isolated from the same patient with 8 years apart.
[f]Strain OMI 1046 and OMI 1104 were isolated from the same patient with 8 years apart.
[g]Strain OMI 1079 and OMI 1101 were isolated from the same patient with 8 years apart.
[h]The exact date of isolation was unknown but suspected based on information of related publications.

20411014, 2023, 5, Downloaded from https://onlinelibrary.wiley.com/doi/10.1111/omi.12433 by Cochrane Germany, Wiley Online Library on [04/12/2023]. See the Terms and Conditions (https://onlinelibrary.wiley.com/terms-and-conditions) on Wiley Online Library for rules of use; OA articles are governed by the applicable Creative Commons License

TABLE 2 Primer and PCR conditions used for analysis.

Primer	Sequence	Annealing temperature (°C)/time (s)	Amplicon length (bp)
fimAnewF	5t'-TATgCAAgACAATCTCTAAATgg-3t'	50/40	1160[a] or 1070[b]
fimAunivF	5t'-AAgTTTTTCTTgTTgggACTTgC-3t'	55/30	
fimAunivR	5t'-AACCCCgCTCCCTgTATTCCgA-3t'	50/40[a] or 55/30[b]	
fimAVF1	5t'-CCCAACAgTCTCCTTgACAgTg-3t'	57/30	462
fimAVR1	5t'-TATTgggggTCgAACgTTACTgTC-3t'		
fimB-productF	5t'-gAAACAgCCAATgTgCAAARCgTCA-3t'	60/30	357
fimB-productR	5t'-ggCCAggCCggTATAAgTgTCggg-3t'		
fimB-NON-productF	5t'-gAAACAgCCAATgTgCAAARCgTCT-3t'	60/30	357
fimB-NON-productR	5t'-ggCCAggCCggTATAAgTgTCggT-3t'		

[a]Combined with fimAnewF.
[b]Combined with fimAunivF.

2.2 | Preparation of the DNA

After cultivation on TSBA, colonies were suspended in 1 mL saline solution, washed, and bacterial genomic DNA was extracted using the spin column method in accordance with the manufacturer's instructions (QIAamp DNA Mini Kit; Qiagen). The concentration and purity of DNA were determined photometrically (NanoVue Plus Spectrophotometer, GE Healthcare Europe GmbH). Our 34 isolates had a minimum DNA concentration of 28 ng/μL and purity within the normal range (260/280 nm of 1.8-2.0). Subsequently, the extracted DNA was used to detect the *fimA* and *fimB* genes by PCR and gel electrophoresis. The location of the *fimA* and *fimB* genes in the long fimbrial gene cluster and the transcriptional organization of this locus are shown in Figure S2A.

2.3 | PCR amplification of *fimA*

For the amplification of *fimA*, the new universal forward primer fimAnewF (5′-TATgCAAgACAATCTCTAAATgg-3t') was developed, which targets the gene upstream to *fimA* (*pgn_0179*) (Table 2). The gene *pgn_0179* may be important for the assembly of FimA monomers (Xu, 2010). Together with the universal reversed primer fimAunivR (5′AACCCCgCTCCCTgTATTCCgA-3t'), designed by Enersen et al. (2008), this primer pair generated an 1160-bp amplicon for the human isolates covering the entire *fimA* including signal sequence and C19-lipidation site but failed with respect to the animal isolates. Further *fimA* genes from animal strains for contrast and evolution studies could only be amplified by combining the established primer pair (fimAunivF; Shimoyama et al., 2017/fimAunivR; Enersen et al., 2008) while omitting the signal sequence (1070 bp as reduced length). It should be noted that another *fimA*-directed universal forward primer "unifim2F" published (Enersen et al., 2008) is located in the center of *fimA* (420 bp downstream the start codon) and has still to be inverted and complemented before creating PCR products combined with fimAunivR. All primers were synthesized by TIB Molbiol Syntheselabor GmbH (Berlin) (see Table 2 for an overview).

2.4 | PCR protocol

Note that 0.5 μL of forward and reverse primer each (100 μM) were combined with 0.5 μL of undiluted DNA, 5 μL of 10X PCR buffer (1.5 mM $MgCl_2$), 2.5 μL of a dNTPs mix (2 mM), 0.5 μL of Taq DNA polymerase (0.5 units), and 40.5 μL of nuclease-free water, resulting in a reaction volume of 50 μL (all PCR reagents by Roche). The PCR reaction was performed in a MicroAmp reaction tube (Applied Biosystems) placed in a PCR Express Thermal Cycler (Thermo Hybaid). The cycling parameters used were as follows: initial denaturation at 95°C for 2 min; 35 cycles; per cycle denaturation at 95°C for 30 s, primer annealing according to Table 2, and for elongation 72°C for 90 s; final elongation at 72°C for 10 min. A positive control (DNA of reference strains) and a negative control (water without any DNA) were always included in the PCR.

2.5 | Specific *fimA* subtype V-directed PCR

Our entire *P. gingivalis* strain collection of about 160 isolates was further screened for the presence of *fimA* subtype V strains, as this is particularly rare and under-investigated on all levels (genotype/phenotype, virulence, clinical implications). For such a PCR-based screening, the primer "fimAVF1" (5t'-CCCAACAgTCTCCTTgACAgTg-3t') was combined with the primer "fimAVR1" (5t'-TATTgggggTCgAACgTTACTgTC-3t') designed by Nakagawa et al. (2000) (Table 2) and applied to genomic DNA pooled from 5 to 10 strains. These primers target a specific nucleotide sequence within the *fimA* gene proven to be unique to subtype V. Conditions for the *fimA* subtype V PCR were identical to those for the universal *fimA* PCR, and annealing conditions are shown in Table 2.

20411014, 2023, 5, Downloaded from https://onlinelibrary.wiley.com/doi/10.1111/omi.12433 by Cochrane Germany, Wiley Online Library on [04/12/2023]. See the Terms and Conditions (https://onlinelibrary.wiley.com/terms-and-conditions) on Wiley Online Library for rules of use; OA articles are governed by the applicable Creative Commons License

2.6 | PCR amplification of *fimB*

For the demonstration of a functional *fimB* gene or presence of an internal stop codon leading to a truncated, very probably non-functional FimB anchor protein, two new primer pairs were developed: either positive in case of a functional FimB: fimB-productF (5t'-gAAACAgCCAATgTgCAAARCgTCA-3t') combined with fimB-productR (5t'-ggCCAggCCggTATAAgTgTCggg-3t'); or positive in case of an irregular *fimB* gene with an internal stop codon: fimB-NON-productF (5t'-gAAACAgCCAATgTgCAAARCgTCT-3t') combined with fimB-NON-productR (5t'-ggCCAggCCggTATAAgTgTCggT-3t') (Table 2). The PCR amplification conditions for the regular and irregular *fimB* gene were identical to the conditions mentioned above, with the exception of annealing conditions that are shown in Table 2. The importance of FimB in the assembly of fimbriae is shown in Figure S2B. The fimbriae of *P. gingivalis* are assembled by a process known as protease-mediated polymerization and are therefore classified as type V pili, which should not be confused with the subtype V.

2.7 | Analyzing the *fimA* sequence and translation into protein sequences

All PCR products were purified in accordance with the manufacturer's instructions (NucleoSpin Gel and PCR Clean-up). The purified DNA was sent for Sanger sequencing (Eurofins Genomics). For the sequencing reaction, 5 μL of each PCR product (20–80 ng/μL) and 5 μL of diluted primer (5 μM = 5 pmol/μL) were pipetted into a 0.5-mL Eppendorf tube (Applied Biosystems; Waltham). Based on the overlapping sequencing data of the forward and reverse sequence and by checking chromatograms in case of doubt, we were able to generate ambiguity-free *fimA*/FimA fasta files (the latter after in silico translation) using BioEdit (Version 7.0.5.3) (Alzohairy, 2011). Fasta files of OMI-strains plus corresponding *fimA* (16) or FimA (83) from GenBank (NCBI) were imported into Mega 11 (version 11.0.13) (Tamura et al., 2021), and an alignment was calculated using the ClustalW algorithm. This alignment was further processed by the ClustalOmega program (version 1.2.1) of EMBL (European Bioinformatics Institute) in order to confirm or optimize the results (Sievers & Higgins, 2021). Subsequently, the alignment was reimported into Mega 11, and phylogenetic trees on DNA and the protein level (both with and without signal sequence) were gener- ated using the neighbor-joining (NJ) model (Mihaescu et al., 2009) with bootstraps set to 500 repeats and rooted at the *Porphyromonas gulae* (*fimA* type A) isolates.

2.8 | Electron microscopic examination

The biofilm, bacterial cells, and fimbriae of isolates OMI 1132 (ATCC 33277) and OMI 622 were further examined using a transmission electron microscopy (TEM) and a scanning electron microscopy (SEM). For this purpose, bacteria were cultured under anaerobic conditions in brain-heart infusion (BHI) and Brucella broth medium in 24-well microplates (Thermo Fisher Scientific Inc.) for 5 days. For TEM examination, bacteria were then washed in 0.1 M Hepes buffer and applied to glow-discharged nickel grids coated with Formvar carbon (Maxtaform, 200 mesh, Science Services GmbH). After washing with distilled water, negative staining was performed with 1% phosphotungstic acid (diluted in bidistilled water; Science Services GmbH). Samples were examined using a Hitachi HT7800 TEM (Hitachi) operating at an acceleration voltage of 100 kV. For SEM, bacteria were fixed with 3% (vol/vol) glutaraldehyde (Agar Scientific) in 0.1 M Soerensen's phosphate buffer, washed in phosphate buffer for 15 min, and dehydrated by incubating consecutively in an ascending ethanol series (30%, 50%, 70%, 90%, and 100%) for 10 min each and the last step thrice. The samples were critical point dried in liquid CO_2 (Polaron, GaLa Instrumente) and sputter coated (Sputter Coater EM SCD500; Leica) with a 10-nm gold/palladium layer. Samples were analyzed using an SEM Quattro S (Thermo Fisher) with a 10-kV acceleration voltage in a high vacuum environment.

3 | RESULTS

3.1 | Amplification of the *fimA* and *fimB* gene

For 34 *P. gingivalis*-related isolates (including human and animal strains) from our own collection (OMI), the *fimA* and *fimB* genes were amplified, and the products were analyzed for the intended length by agarose gel electrophoresis and sequenced, exemplarily in the case of *fimB*. Applying the new combination of primers fimAnewF/fimAunivR, we were able to amplify the entire *fimA* gene including leader (summing up to 1160 bp) for each of the 28 human isolates tested. However, this primer pair failed to amplify *fimA* of sheep and jaguar strains or revealed only weak bands in the case of cat, dog, or monkey strains. To amplify most *fimA* of animal strains, the established primer pair fimAunivF (Shimoyama et al., 2017) plus fimAunivR (Enersen et al., 2008) was successful while omitting the signal sequence (amplicon 90 bp shorter). In this way, however, sequences could be obtained for 6/9 animal isolates (four monkeys, one each from cats and dogs), but for the remaining three animal isolates (two sheep and one jaguar isolate), only a weak amplicon could be generated, which was not sufficient for ambiguity-free sequencing. While the six isolates were members of *P. gulae* (the nearest known neighbor of *P. gingivalis*), sheep isolates were identified as *Porphyromonas loveana* and the jaguar isolate as *Porphyromonas circumdentaria*, and we decided not to investigate these strains any further. For the 34 *fimA*-positive isolates, we also attempted to amplify the *fimB* gene. The *fimB* gene can occur in two different alleles. In the very common and functional variant, *fimB* encodes a lipoprotein anchor component (FimB) of the major fimbriae that–if bound to the last FimA–terminates polymerization and defines pilus length (Figure S2B). The second variant contains an internal stop codon that results in a missing or truncated and most probably non-functional FimB anchor protein. Therefore, two new primer pairs were designed, either positive without (switch y/n, regular) or with the internal stop codon (switch n/y, truncated). Each of the 34 isolates was tested with

20411014, 2023, 5, Downloaded from https://onlinelibrary.wiley.com/doi/10.1111/omi.12433 by Cochrane Germany, Wiley Online Library on [04/12/2023]. See the Terms and Conditions (https://onlinelibrary.wiley.com/terms-and-conditions) on Wiley Online Library for rules of use; OA articles are governed by the applicable Creative Commons License

both primer pairs (Figure S2C). For 33 isolates including strain 381, which is a progeny of ATCC 33277, a regular *fimB* gene was amplified. These isolates showed switch y/n. In contrast, the type strain ATCC 33277 showed switch position n/y (stop codon, truncated FimB). Thus, FimB truncation is a special feature of ATCC 33277 (but not of 381), which is in accordance with database entries NZ_CP025930.1 resp. NC_010729.1 (both ATCC 33277), NZ_CP012889.1 (381), and Coats et al (2019) but in contrast to publications of the Nagano-group (Hasegawa & Nagano, 2021; Nagano et al., 2010). The discrepancy, however, could also be due to ongoing AAA/TAA transversions between subcultures. Sequencing *fimB* in two strains (381, W83) confirmed the identity and sequence homogeneity outside primer regions.

3.2 | Phylogenetic trees and subtype-classification

After amplification, *fimA* of all 28 human and six animal isolates could be sequenced ambiguity-free, and results were combined in a first alignment with another 16 *fimA* reference sequences of genotypes I-V available by GenBank. Based on these 50 *fimA* nucleotide sequences, we constructed a neighbor-joining phylogenetic tree showing eight genotypic clusters A-H in total (Figure 1 with signal sequence, Figure **S3A** without signal sequence, Figure **S3B** as phylogram with scale bar). One strain, OMI 1077 (Canada), was located between clusters D and E and classified as "hybrid." Hybrids are rare strains that are phylogenetically located between true clusters (as outliners) with the restriction that this definition requires a sufficiently large quantity of recorded and sequenced strains (Conrads et al., 2017).

In the next step, we translated the complete *fimA* nucleotide sequences of these 50 strains in silico into the corresponding amino acid sequences and combined them with FimA sequences of another 83 strains available by GenBank of NCBI in a second alignment. In summary here, 34 isolates were new, sequenced, and translated; 16 were imported at the DNA level and translated; and 83 were imported at the protein level (99 imported sequences in total, 133 sequences in total). Based on this amino acid sequence alignment, three phylogenetic trees for FimA "serotypes" (Figure **2** with signal sequence, Figure S3C without signal sequence, Figure S3D as phylograms with scale bar) were constructed. Of note, we prefer the term "serotype" since it is an alignment at the protein level, wise to the fact that a serotype would have to be confirmed via the reaction with antibodies.

The NJ-cladograms and NJ-phylograms of 50 *fimA* genotypes and 133 FimA serotypes all showed the same eight distinct clusters A-H along with some outliners (possibly hybrid strains) corresponding to type A of *P. gulae* and seven human *fimA*/FimA *P. gingivalis* subtypes, including two II-subtypes (a and b) for nomination.

Cluster A, containing all six *P. gulae* animal isolates with *fimA* type A (Fujiwara-Takahashi et al., 2020). We hereby propose that it possibly represents the ancestral sequence of the *fimA* gene as frequently found and especially in monkeys. However, it is known that several animal lineages (type B and C) exist, and horizontal *fimA* gene transfer between several genotypes of *P. gingivalis*/*P. gulae* is possible and probably ongoing (Fujiwara-Takahashi et al., 2020).

Cluster B contains two sequences from rural isolates in Indonesia (OMI 1088 and 1127) and the current serotype Ib (HG1691 related).

Cluster C corresponds to the current serotype I, including various ATCC 33277 *fimA* sequences slightly different depending on the source.

Especially the phylograms (Figure S**3B,D**) show a close relationship between serotype I/Ib and type A. Together, serotypes I/Ib were found in 42 isolates and thus in 31.6% of all strains examined. We believe that this high frequency and richness of variants could possibly indicate a greater phylogenetic age.

Between Clusters B and C (I/Ib), two hybrid strains were identi- fied (sequences WP 097638037.1, BAN288833.1) labeled in gray, as all outliners throughout our phylogenetic trees.

Clusters D and E correspond to the current subtype II, which has not been further differentiated into sub-serotypes before. We hereby suggest differentiating serotype II into subtypes IIa (containing all currently known references: HW24D1, OMZ314, OMZ409, and TDC285) and IIb (containing among others TDC60 sequences and four strains of our collection). Of note, at least in one cluster analysis (Figure **S3C**), subtype IIb was even closer related to subtype III than to subtype IIa further indicating the need for separation. Serotypes IIa/IIb occurred in 43 isolates (32%).

Cluster F represents the current serotype III, including reference strains ATCC 49417 by several sequences from different laboratories and BH6/26. A link has been found to serotype B of *P. gulae* (Fujiwara-Takahashi et al., 2020).

Between Clusters C and D (between serotypes I and II), five hybrid strains were identified (strain KUMCP5 and sequences WP 234241607, 211599903.1, 099810698.1, and 097548069.1). In addition, four outliners (OMI 1077 as well as WP 097632920.1, 054191214.1, and 088492431.1) were located between serotypes II and III (Clusters E and F).

Cluster G represents serotype IV known for enhanced vir- ulence and contains several sequences from W83, W50 (WP_005873481), and HG564. This cluster is highlighted in red. A link has been found to serotype C of *P. gulae* (Fujiwara-Takahashi et al., 2020).

Although serotypes III and IV contain subclusters, they present themselves relatively homogeneous compared to types I and II, so that further differentiation appears superfluous. Both types seem to be rarer, with serotype III occurring in 19 (14%) and serotype IV in 17 (13%) isolates.

20411014, 2023, 5, Downloaded from https://onlinelibrary.wiley.com/doi/10.1111/omi.12433 by Cochrane Germany, Wiley Online Library on [04/12/2023]. See the Terms and Conditions (https://onlinelibrary.wiley.com/terms-and-conditions) on Wiley Online Library for rules of use; OA articles are governed by the applicable Creative Commons License

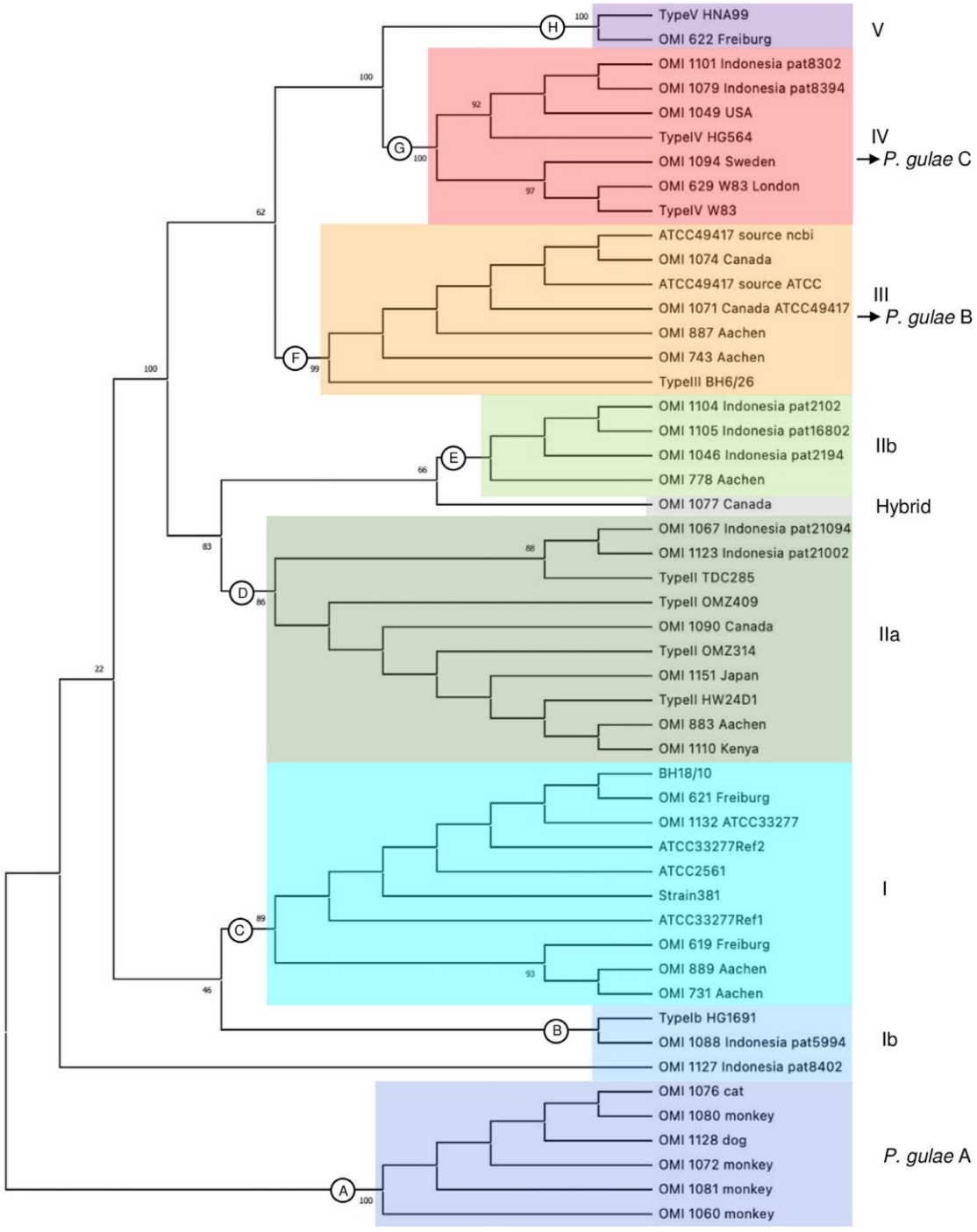


FIGURE 1 Neighbor-joining phylogenetic tree (cladogram) based on *fimA* genotypes (with signal sequence) of 50 *P. gingivalis* strains.

Finally, Cluster H corresponds to the current serotype V (strain HNA99 as reference) and contains no subtypes. Serotype V is rarely found (4%). Fortunately, in our collection, we found a single isolate (OMI 622, origin Freiburg, Germany) expanding the small collection worldwide.

Overall, serotypes I and II proved to be the dominant subtypes and serotype V the rarest. The prevalence of serotypes is consistent with results from other studies (Beikler et al., 2003; Enersen et al., 2008; Nakagawa et al., 2000).

Of note, the reference strain ATCC 49417 is deposited as serotype II in the NCBI database but as serotype III in the ATCC database. This led to misleading information in publications (Beikler et al., 2003; Nakagawa et al., 2000). In our phylogenetic tree, the strain is in cluster F, which corresponds to serotype III. ATCC 49417 is much more closely related to the serotype III reference strain BH6/26 than to the reference sequences for serotype II.

20411014, 2023, 5, Downloaded from https://onlinelibrary.wiley.com/doi/10.1111/omi.12433 by Cochrane Germany, Wiley Online Library on [04/12/2023]. See the Terms and Conditions (https://onlinelibrary.wiley.com/terms-and-conditions) on Wiley Online Library for rules of use; OA articles are governed by the applicable Creative Commons License

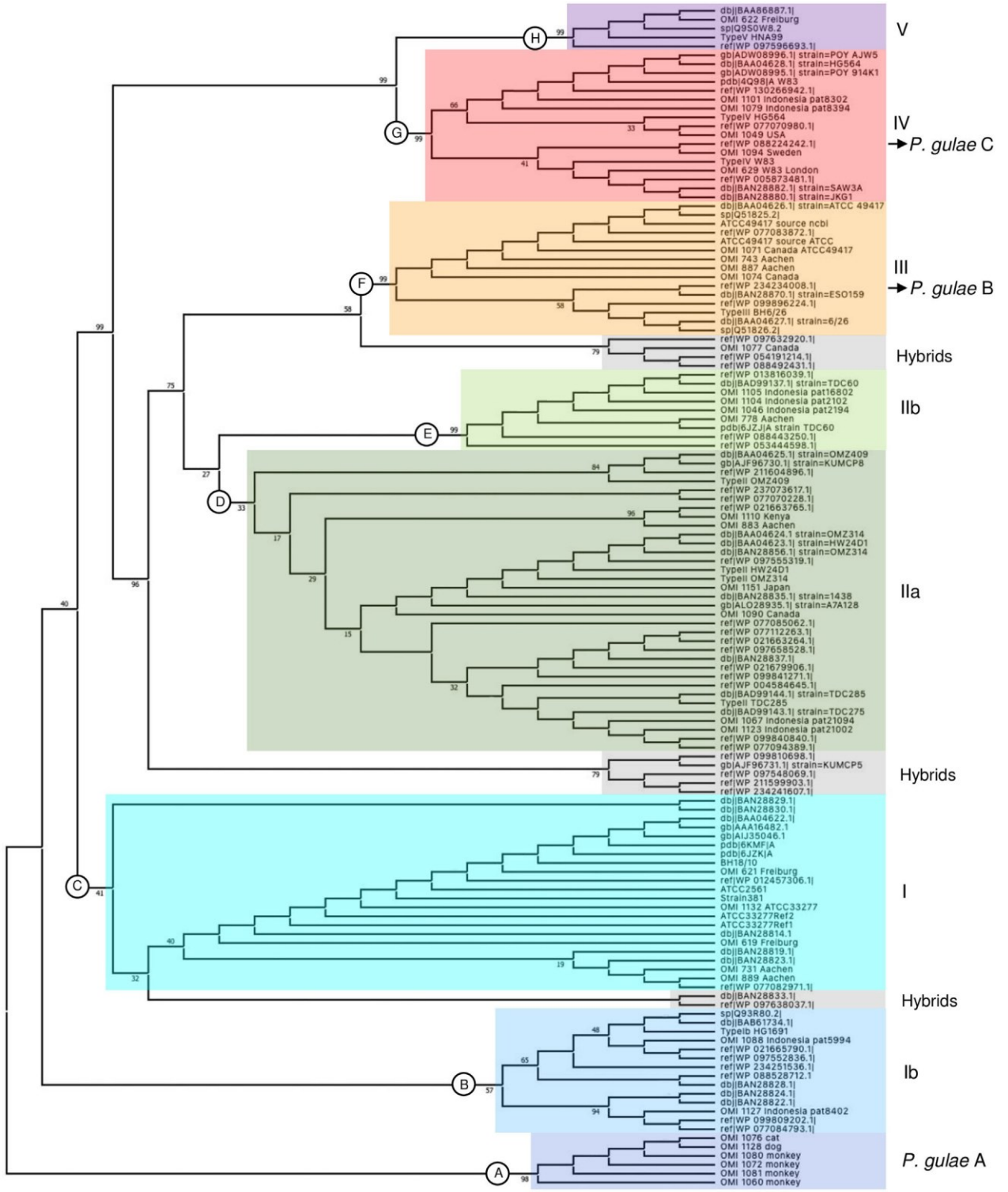


FIGURE 2 Neighbor-joining phylogenetic tree (cladogram) based on FimA serotypes (with signal sequence) of 133 *P. gingivalis* strains.

3.3 | Assembly and function of the FimA protein

The importance of certain amino acid exchanges (plus insertions/deletions) between the sub-serotypes becomes clear when the functional domains for polymerization and interaction with the environment (host) of the FimA monomer are studied in detail. For background information, we provide a little summary of "Assembly and function of the FimA protein" in the Supporting Information. Below, we present the results of the comparison at the amino acid sequence level.

20411014, 2023, 5, Downloaded from https://onlinelibrary.wiley.com/doi/10.1111/omi.12433 by Cochrane Germany, Wiley Online Library on [04/12/2023]. See the Terms and Conditions (https://onlinelibrary.wiley.com/terms-and-conditions) on Wiley Online Library for rules of use; OA articles are governed by the applicable Creative Commons License

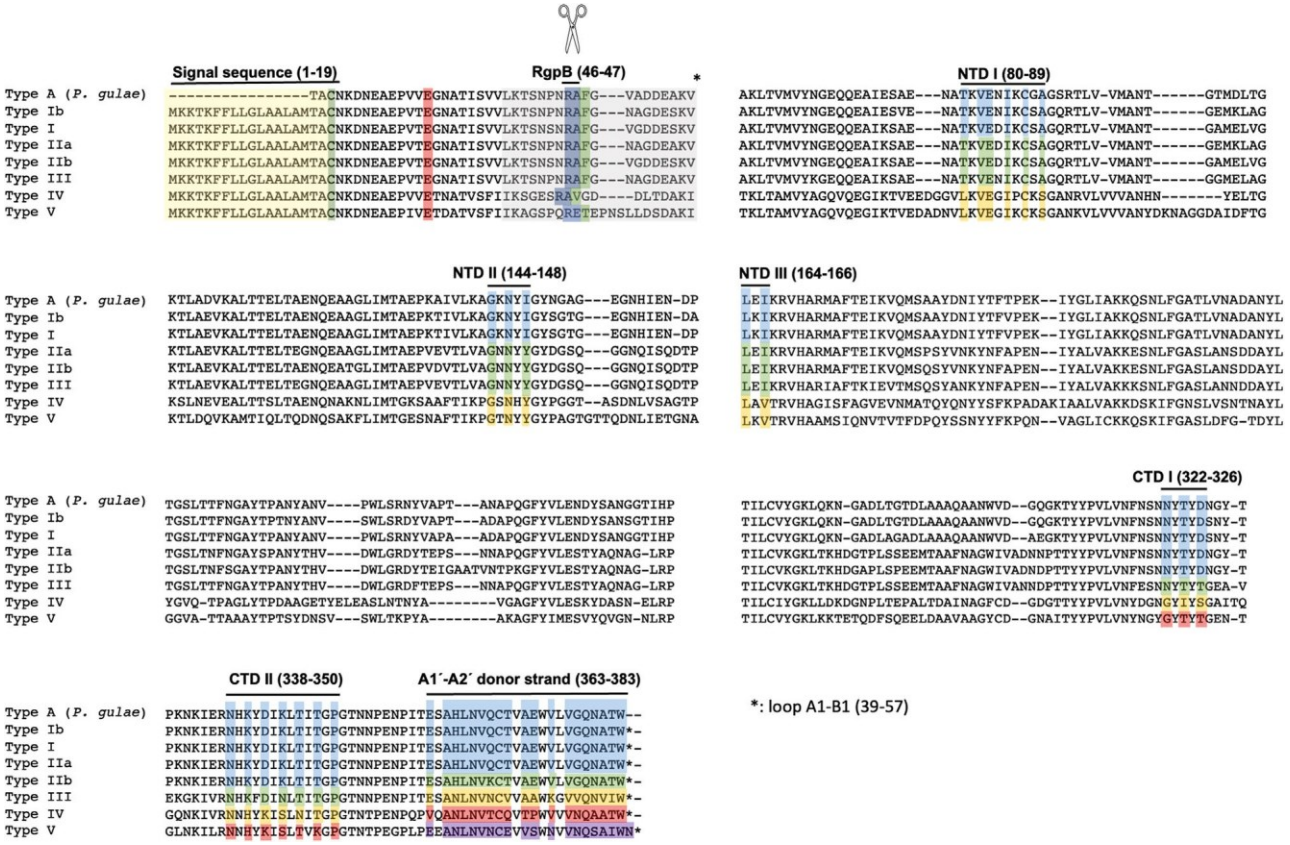


FIGURE 3 Assignment of regions that control the polymerization of FimA. Sequences that are important for transport, membrane integration, processing, and polymerization are marked with a horizontal black bar and highlighted in color. These include the signal sequence (1-18 plus C19-lipidated), the RgpB cleavage site (46-47), the A1-B1 loop (39-57, light gray), an N-terminal part (NTDI 80-89, NTDII 144-148, NTDIII 164-166), and a C-terminal part (CTDI 322-326, CTDII 338-350) of the hydrophobic groove as well as the A1'-A2' donor strand (363-383). The strains representative for the subtypes were OMI 1080 monkey (*P. gulae*, type A), OMI 1127 Indonesia pat8402 (Ib), ATCC 33277 (I), OMI 883 Aachen (IIa), OMI 1105 Indonesia pat16802 (IIb), OMI 887 Aachen (III), W83 Bonn (IV), and HNA99 (V).

3.4 | Amino acid changes with consequences on polymerization

The important structures for the polymerization of FimA can be deduced from the three-dimensional crystal structure (fig. 1b in Shibata et al., 2020) and online via rcsb.org/structure/6KMF. Thus, an exact assignment of individual amino acids to polymerization is possible. Shibata et al. (2020) already showed that amino acid sequences in functional regions vary between subtypes I-V, possibly resulting in different three-dimensional tertiary structures of the fimbrial protein. As a significant enhancement of our study, we expanded this domain-specific alignment of five types to seven human subtypes along with *P. gulae* type A.

Figure 3 shows the 100% conserved signal sequence (1-19, yellow label, from M1 to lipidated-C19). The missing sequence of type A is due to the different primer pair used for successful amplification of *P. gulae*. This is in contrast to other bacteria where the signal peptide of pili is less conserved (Enersen et al., 2013). In all serotypes, the mature FimA monomer used to assemble the fimbriae thus starts with amino acid E30 (marked in red). In a closed configuration of the FimA monomer, the donor strand A1'-A2' (see fig. 1 in Shibata et al., 2020, marked in red also) is located below the N-terminal loop A1-B1 (marked in blue). The scissors in Figure 3 (as in Shibata et al., 2020) mark the RgpB cleavage site at the N-terminal loop A1-B1. Corresponding amino acid sequences are also marked in Figure 3. Loop A1-B1 is located at the N-terminal start (between amino acids L39 and V57, light gray), and donor strand A1'-A2' is located at the C-terminal end (between amino acids E363 and W383). The RgpB cleavage site is located between amino acids R46 and A47. After cleavage, the FimA monomer is activated, and the donor strand A1'-A2' is released. Simultaneously, in place of the released donor strand, a hydrophobic groove is created in the protein. If the A1'-A2' strand of a neighboring monomer (floating in the same membrane) is activated, two FimA monomers can be coupled. During this process, the A1' part of the A1'-A2' strand binds into an N-terminal part (NTD) of the hydrophobic groove. Correspondingly, the A2' part binds into a C-terminal part (CTD). These TD structures are also marked in Figure 3. Interestingly, we found that the RgpB cleavage site between amino acids R46 and A47 is conserved among all types except type V in which glutamic acid (E) is located at position 47 (E47). As was shown before, substituting the kind of amino acid neighboring arginine (R) at the cleavage site (P1 and P2 positions) will alter the kinetics of substrate digestion (Ally et al., 2003), in the case of FimA

20411014, 2023, 5, Downloaded from https://onlinelibrary.wiley.com/doi/10.1111/omi.12433 by Cochrane Germany, Wiley Online Library on [04/12/2023]. See the Terms and Conditions (https://onlinelibrary.wiley.com/terms-and-conditions) on Wiley Online Library for rules of use; OA articles are governed by the applicable Creative Commons License

most likely influencing both, the speed and final length of polymerization. The adjacent amino acids at position 48 (P3 position) are also color-coded (green) in Figure 3. Subtypes A, I, Ib, IIa-b, and III have a nonpolar phenylalanine (F) at this position, while subtype IV has a nonpolar valine (V), and subtype V has a polar threonine (T), both of which may also lead to altered enzymatic activity. Further, aa sequence variations between subtypes occur in other regions important for the polymerization of FimA. As further shown in Figure 3, the N-terminal part (NTD) and the C-terminal part (CTD) of the hydrophobic groove each consist of individual sequence segments (NTD I-III and CTD I-II, respectively) that join to form a beta-sheet. For example, subtypes A, I, Ib, IIa-b, and III have a threonine (T) in NTD I at position 80, whereas subtypes IV and V have a leucine (L). Similarly, subtypes A, I, Ib, IIa-b, and III have an alanine (A) at position 89, while subtypes IV and V have a serine (S). These differences continue in the CTDI and II regions as well as for the A1'-A2' donor strand sequence and are each highlighted by a different colored background. It is likely that these differences result in altered folding of the beta-sheet and hydrophobic groove. Therefore, the nomination of additional subtypes seems to be justified. The differences between subtypes IIa and IIb are evident at position 370 in the A1'-A2' donor strand region. Here, subtype IIa has a Q (glutamine, polar uncharged), whereas subtype IIb has a K (lysine, positively charged). Types A, I, and Ib, however, cannot be distinguished at this site and have identical hydrophobic grooves. The distinction of subtypes IIa-b, III, IV, and V again becomes clear at position 372, where subtypes II a-b have a glutamic acid (E, negatively charged), subtype III an alanine (A, hydrophobic), subtype IV a proline (P, hydrophobic, helix disruptor), and subtype V a serine (S, polar uncharged).

3.5 | Amino acid changes with consequences on microbe-host interactions

FimA has regions that act as immune epitopes. These include a binding site for CD14, which is labeled in Figure 4 between aa 115 and 136. CD14 is expressed primarily by macrophages and monocytes and plays a role in the nonspecific immune system in recognizing bacteria by binding to lipopolysaccharides of Gram-negative bacteria. Another region that acts as an immune epitope is the binding site for CD11b/CD18 (aa 212-231 and aa 252-274). CD11b/CD18 is also known as complement receptor 3 through which the uptake of microorganisms into macrophages is mediated. The eight subtypes from our phylogenetic tree showed different aa sequences within these regions, possibly resulting in an altered interaction with the immune system. In Figure 4, 5, all positions where amino acids differ between subtypes are again color-coded and categorized. The differences between the previous subtypes I, Ib, II, III, IV, and V can already be recognized relatively clearly by the coloring. However, there are also small other differences between the additional subtypes A, IIa, and IIb that we distinguish. Subtype A of animal isolates has an asparagine (N, polar uncharged) at position 257 in the CD11b/CD18 II domain, whereas subtypes Ib and I have both an aspartic acid (D, negatively charged). At position 252 in the CD11b/CD18II domain, subtype I has an alanine (A, hydrophobic), while subtypes A and Ib have a threonine (T, polar uncharged). At position 123 in the CD14 domain, subtypes IIa and III have a glycine (G) with no side chain, whereas subtypes IIb, A, I, Ib, and IV have glutamic acid (E, negatively charged). The distinction between subtypes III, IV, and V is evident at several locations, for example, at position 119 in the CD14 domain, where there is a switch from the acidic glutamic acid (E) of type III to the polar uncharged serine (S) of type IV or glutamine (Q) of type V. The classification of aa pattern subtypes as "serotypes" might thus be justified as the related immunogenicity might vary. In addition and as we propose, the need for further differentiation between subtypes IIa-b becomes apparent. Other functional regions of the FimA protein interact with salivary proteins. A general binding site is located between aa Y312 and 333. In addition, there are specific and overlapping binding sites for statherin (aa 339 to 372) and PRP1 (aa 364 to W383). The subtypes also differ significantly in these regions indicating a different interaction with host proteins. In the functional regions interacting with salivary proteins, subtypes A, I, Ib, IIa, and IIb are very similar in structure, whereas subtypes III, IV, and V can be distinguished at different positions. Similarly, at position 370 in the region shared by statherin/PRP, these subtypes do have a threonine (T, polar uncharged), whereas subtype III has a valine (V, hydrophobic), subtype IV glutamine (Q, polar uncharged), and subtype V glutamic acid (E, negatively charged). The distinction between subtype IIa and IIb, however, becomes evident at position 368. Here, subtype IIa (together with A, I, Ib) has a glutamine (Q, polar uncharged), whereas subtype IIb has a lysine (K, positively charged). Even subtypes III, IV, and V are closer related to IIa, as having polar amino acids (asparagine: subtypes III and V, threonine: subtype IV).

3.6 | Electron microscopic examination

The long fimbriae of isolates OMI 1132 (ATCC 33277, fimbriae subtype I) and OMI 622 (subtype V) were further examined after growing strains in two different media (BHI or Brucella broth) in microtiter plates and using both TEM and SEM. The results are shown in Figure 5. While in most images and excerpts 3 nm wide single, distinct fimbriae could be observed, there were also excerpts with initial bundling of sev- eral long fimbriae, braid-formation (up to 50 nm wide) (Figure 5A) and mesh-formation and even brick-work-like structures to observe. To the best of our knowledge, Figure 5 (with more details in Figures **S4A**) is the first close-up image of the long (bundled) fimbriae of *P. gingivalis*. The only microscopic image to date that demonstrates bundling and–as a further consequence–"brickwork formation" in *P. gingivalis* was published by an Australian group (Zhu et al., 2013).

4 | DISCUSSION

In this study, we have gained new insights into the diversity of FimA and–more limited–FimB in a variety of *Porphyromonas* strains, isolated from both humans and animals. We have constructed phylogenetic trees based on *fimA* and FimA sequences. The current classification

20411014, 2023, 5, Downloaded from https://onlinelibrary.wiley.com/doi/10.1111/omi.12433 by Cochrane Germany, Wiley Online Library on [04/12/2023]. See the Terms and Conditions (https://onlinelibrary.wiley.com/terms-and-conditions) on Wiley Online Library for rules of use; OA articles are governed by the applicable Creative Commons License

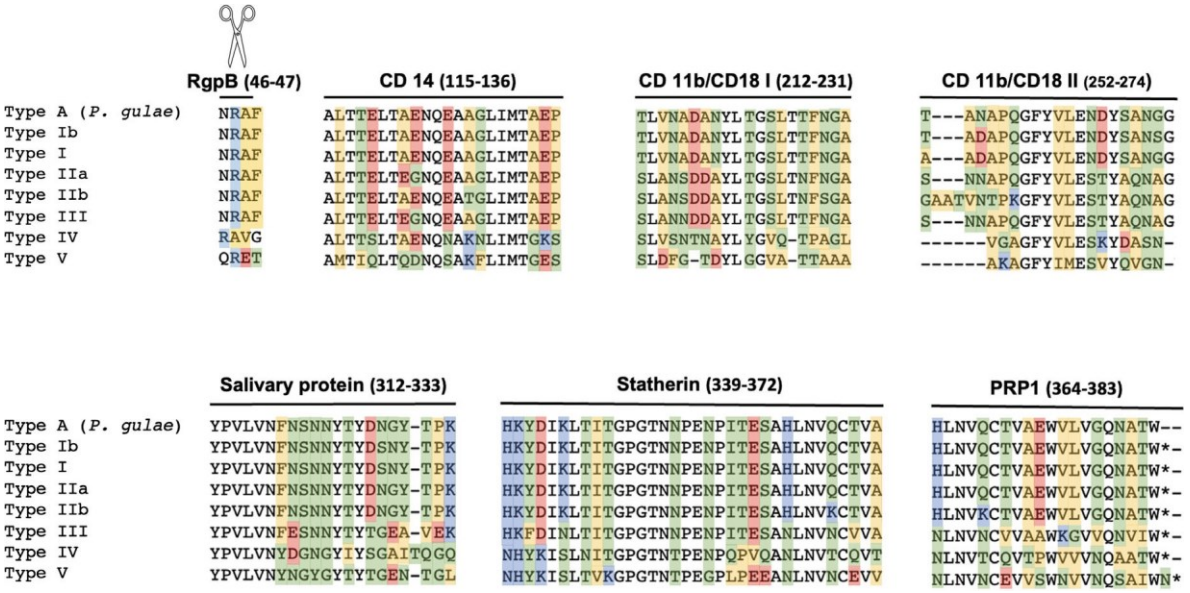


FIGURE 4 Classification of amino acids in the functional regions of FimA. Positions where amino acids differ between subtypes are marked in color. Non-polar amino acids are highlighted in yellow, polar amino acids in green, basic amino acids in blue, and acidic amino acids in red. The strains representative for the subtypes were OMI 1080 monkey (*P. gulae*, type A), OMI 1127 Indonesia pat8402 (Ib), ATCC 33277 (I), OMI 883 Aachen (IIa), OMI 1105 Indonesia pat16802 (IIb), OMI 887 Aachen (III), W83 Bonn (IV), and HNA99 (V).

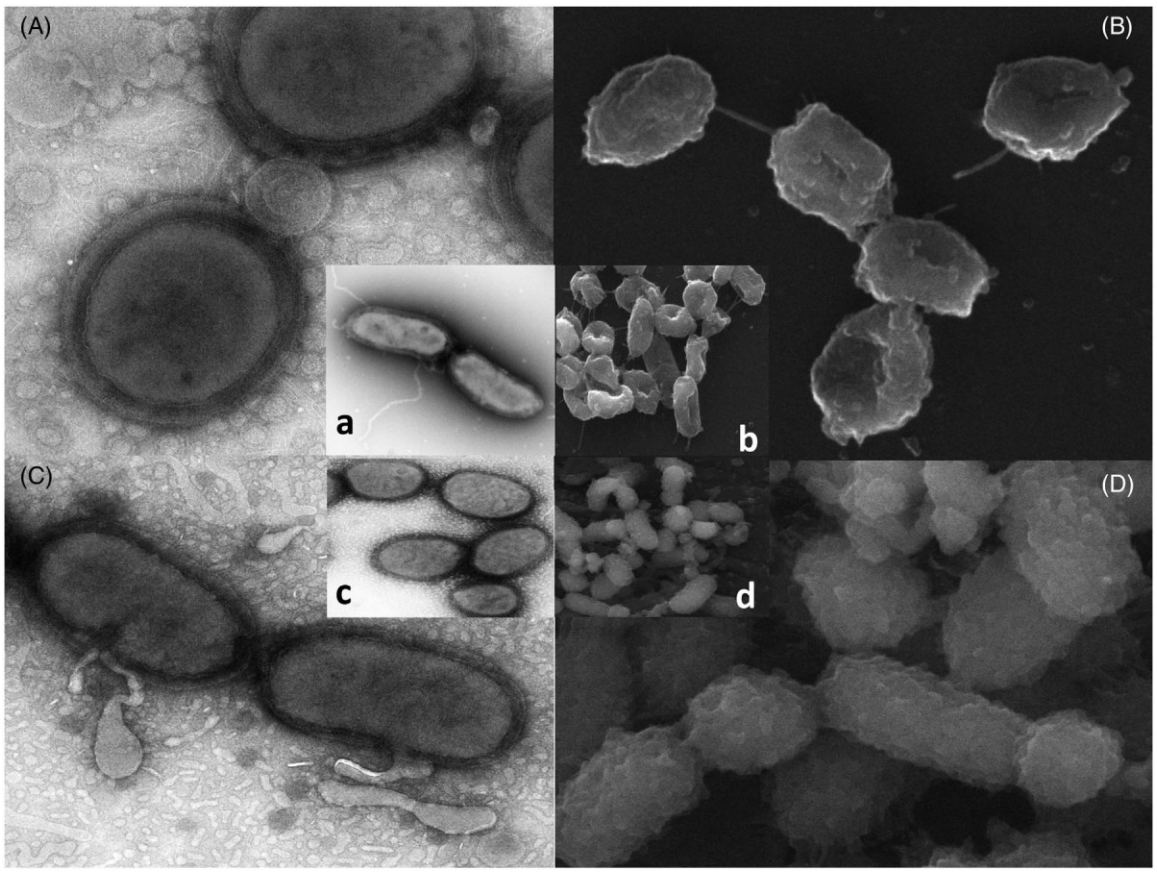


FIGURE 5 Transmission electron microscopy (TEM) (left, A, C) and scanning electron microscopy (SEM) (right, B, D) pictures of fimbrial type I strain *P. gingivalis* ATCC 33277 (upper, A, B) and of fimbrial type V strain OMI 622 (lower, C, D). Strain ATCC 33277 shows very long, partially bundled fimbriae demonstrated in TEM (A, a) and SEM (B, b). OMI622 rarely showed any long fimbriae in TEM (C, c) or SEM (D, d). Instead, intensified vesicle production leading to a slimy appearance was apparent in OMI 622. Be aware that B-b, C-c, and D-d were made from the same preparations, while A-a originated from different samples. For more details, see Figure 4A,B.

20411014, 2023, 5, Downloaded from https://onlinelibrary.wiley.com/doi/10.1111/omi.12433 by Cochrane Germany, Wiley Online Library on [04/12/2023]. See the Terms and Conditions (https://onlinelibrary.wiley.com/terms-and-conditions) on Wiley Online Library for rules of use; OA articles are governed by the applicable Creative Commons License

should be reformed by splitting serotype II into two distinct subtypes IIa and IIb, with the latter closer to subtype III.

4.1 | Traditional *fimA* genotyping by short fragment PCR versus complete *fimA* sequencing

Up to now, the *fimA* gene has been divided into six subtypes (I, Ib, II, III, IV, and V), based on variations in its nucleotide sequence in very short, selected regions covered by type-specific primers (Amano et al., 1999; Fujiwara et al., 1993; Nakagawa et al., 2000, 2002). Only in the case of subtypes V and Ib, two specific primers were applied, while for all others, a shared reversed primer was used. This method and the classification derived from it, which was still innovative at the time of introduction (Beikler et al., 2003; Enersen et al., 2008), is insufficient from today's point of view, as it leads to many cross-reactions between types and a typing scheme full of false type I-II-III hybrids, which can easily be confused with the real hybrids (outliners) existing. For instance, Enersen et al. described eight isolates being a combination of genotypes I, Ib, and II and four isolates combining genotypes I-II. In addition, strains that could not be typed were found in various studies (Beikler et al., 2003; Enersen et al., 2008; Nakagawa et al., 2000, 2002). A clear relationship between the *fim*-genotype and virulence could not yet be shown and rather contradictory results are available. Isolates with *fimA* genotypes Ib, II, and IV were found to cause more severe infectious symptoms and inflammatory changes than strains with genotypes I and III. Several human studies supported the view that fimbriae of types II and IV are a critical determinant of virulence. In patients with chronic marginal periodontitis, it was then found that *fimA* genotype II (followed by Ib and IV) was significantly more common than other genotypes (Beikler et al., 2003; Wang et al., 2020). Genotype II also appears to be more common in aggressive periodontitis (Nakagawa et al., 2000). Further experiments with *P. gingivalis* mutants showed that the replacement of type I *fimA* gene with type II gene resulted in increased bacterial adhesion/invasion of epithelial cells, whereas the replacement of type II with type I resulted in decreased efficiency (Inaba et al., 2008). In addition, the relationship between specific *fimA* genotypes and periodontal health was investigated, and it was found that *fimA* genotypes I (by the exclusion of Ib) and V are most prevalent in *P. gingivalis*-positive healthy adults (Nakagawa et al., 2000). In contrast, Umeda et al. (2006) concluded that there were no significant differences between genotypes in studies of adhesion and invasion of *P. gingivalis* in epithelial cells. Further studies could show that type II virulence is very heterogeneous (Inaba et al., 2008), which could be correlated with the subtypes IIa and IIb we propose here, and that type I also occurs with high frequency in patients with severe periodontitis (Beikler et al., 2003). Another observation is that type I is found much more frequently in Caucasians than in Asians. Beikler et al. (2003) pointed out that this might be due to the PCR method used for testing in Asian countries, which often falsely classifies type I as type II.

Of course, the main reason for contradictory results might be that the overall virulence of a strain depends on the sum and expression of its several virulence factors taken together. But insufficient subtyping of the individual virulence factors certainly exacerbates this problem.

To enhance *fim*-gene associated virulence assessment in future studies, we have introduced a new primer pair and typing scheme based on the entire *fimA*/FimA sequence. We have amplified and sequenced the entire *fimA* gene and–after expanding the data set by all currently (August 2023) publicly available *fimA*/FimA data (summing up to 133 sequences)–found new subtypes within II (IIa, IIb). In addition, all isolates could be typed and assigned to a distinct subtype, with the exceptions of 11 true (as we believe) hybrid or outliner sequences, highlighted in gray throughout all cluster analyses and phylogenetic trees in our study, which could either be explained by in nature or in vitro/in silico recombination. As an important detail, we could show that the classification of reference strain ATCC 49417 in ATCC's gene database as type II is incorrect as it belongs to type III proven for four independently generated sequences. Interestingly, within each supercluster (I, II-III, and IV-V), there is always a splitting between a more (Ib, II, and IV) and a less (I, III, and V) virulent cluster. Taken together, our new typing method may provide a more robust fundament for confirmation and a better understanding of Fim-related virulence.

4.2 | New insights into the evolution of *fimA*/FimA and—corresponding—*P. gingivalis* /*P. gulae* as species

The phylogenetic trees of fimA/FimA may allow an evolutionary interpretation on both gene and species (host) levels. This is an attempt to integrate various literature, including those from veterinary microbiology (Fujiwara-Takahashi et al., 2020; O'Flynn et al., 2015), in order to draw an extended evolutionary picture. *Porphyromonas gingivalis* in humans can be presumed to have evolved from animals, especially monkey strains. FimA found in isolates from monkeys and other animals can be traced to serotype I of human *P. gingivalis*. DNA-DNA homology data and 16S rRNA gene sequence analysis show that the differences between *P. gingivalis* and *P. gulae* are only slight but still sufficient to define two distinct species (Fournier et al., 2001). Possibly, type A of monkey-originated *P. gulae* evolved into Ib and I of human *P. gingivalis*, with type I being less virulent than type Ib and thus probably better adapted (tamed) in humans. Horizontal transmission and vertical forwarding have enabled *P. gingivalis* to prevail against other microorganisms and to control or evade the innate immune response of humans. Subtypes II + III and IV + V probably evolved in separate directions from subtype I and always split into a more (II, IV) and a less (III, V) virulent subtype. More virulent strains are highlighted in red, and less virulent strains in green in phylograms of Figure S3B,D. However, mixed types (hybrids, outliners) do occur between types A (animal) and Ib, between subtypes I, II, and III as well as between subtypes II and III. Further evidence of this evolution is the high diversity within serotypes I and II, whereas "younger" serotypes are less diverse (III and IV) and/or rarer (V), as we speculate. The particularly apathogenic type V, as far as assessable with such a few strains isolated so far, appears to be the youngest in evolutionary terms, being most distant from type

20411014, 2023, 5, Downloaded from https://onlinelibrary.wiley.com/doi/10.1111/omi.12433 by Cochrane Germany, Wiley Online Library on [04/12/2023]. See the Terms and Conditions (https://onlinelibrary.wiley.com/terms-and-conditions) on Wiley Online Library for rules of use; OA articles are governed by the applicable Creative Commons License

I. One reason for their rarity could be their apathogenic nature, so that they do not withstand evolutionary pressure sufficiently and are displaced. Very interesting and outlined by Fujiwara-Takahashi et al. (2020), homologous recombination occurs within *P. gingivalis* or within *P. gulae* (evidence: overall genomotype and *fimA* genotype can vary) but seems to be possible across different bacterial hosts, even today. A remarkable evidence found again by Fuijiwara-Takahashi et al. for the latter is that *P. gulae* FJ70 does not have any typical *P. gulae-fimA* type (A-C) but instead *P. gingivalis-fimA* type II.

4.3 | Assembly of the fimbrial protein involving the entire *fim* gene cluster

The *fimA* gene is located in a gene cluster including *fimB*, *fimC*, *fimD*, *fimE*, *pgmA*, and *fimX* (shown in Figure S2A). The *fimA* (shaft), *fimB* (anchor), and *fimCDE* (tip) genes encode immediate structural proteins of the fimbriae (shown in Figure S2B). Gene *pgmA* and *fimX* appear to have a role in the transcription of *fimA*. Investigation of the heterogeneous virulence of *P. gingivalis* requires detailed, structural, and functional knowledge of the fimbrial proteins in the context of the entire filament. There are indications that the heterogeneous pathogenicity of the bacterium, in addition to the genotype of *fimA*, is related to the various morphological features of the polymerized fimbriae, particularly regarding the length. Initially, it has been assumed that fimbrial length correlates with the *fimA* genotype (Nagano et al., 2010). However, it was then discovered that the fimbriae lengths of strain ATCC 33277 of about 1-1.5 μm are exceptional and not representative of genotype I (Nagano et al., 2010). Thus, it has been assumed that fimbriation, including the length of the FimA-polymer, is controlled by a specific mechanism. This mechanism seems to involve FimB, which is an anchor component for the fimbriae and can restrict fimbrial length (Nagano et al., 2010; Shibata et al., 2020). Basically, the encoding *fimB* is highly conserved (except for a few point mutations) and occurs only in a regular common genotype (Hasegawa & Nagano, 2021). In the *fimB* allele of strain ATCC 33277, but not in strain 381 proven by the study here, however, a thymidine is present at position 355, while in all other *P. gingivalis* strains known so far, an adenine is present. This leads to the formation of a stop codon in strain ATCC 33277 but not in its progeny 381 with consequences for immune-stimulating capacity as demonstrated by Coats et al. (2019). Irritating in this context, the 381 strain investigated by a Japanese group seems to possess the internal stop codon (Hasegawa & Nagano, 2021; Nagano et al., 2010). This discrepancy, however, could be due to ongoing AAA/TAA transversions during sub-cultivation which could be monitored by applying the *fimB*-directed PCR introduced here. The evolutionary reason why ATCC 33277 possesses the stop codon and forms particularly long fimbriae is currently unknown. We examined the 34 *P. gingivalis* strains from our collection with respect to the regular and the irregular (with internal stop codon) *fimB* gene in addition to the *fimA* genotype. We discovered that 33 of the 34 *P. gingivalis* strains had a regular *fimB* gene and confirmed that only ATCC 33277 had an irregular *fimB* gene. Thus, this stop codon seems to be formed by "accident" rather than being selected in evolution, and curing of this accident could be favored over time as probably seen in strain 381.

In several of our TEM/SEM pictures, the initial bundling of long fimbriae, braid-formation, and mesh-formation and even brick-work-like structures could be observed. For a long time known, the bundling/cell-cell knotting of long fimbriae has been a virulence mechanism of EPEC/EHEC and *Salmonella* which enables surface adhesion and co-aggregation (Giltner et al., 2012; Sohel et al., 1993; Xicohtencatl-Cortes et al., 2007). Furthermore, for adhesion to neighboring cells and surface structures, the tip of the fimbriae (which will even after bundling and cell-cell knotting be the terminus we assume), formed by the accessory protein of complex FimC-E, appears to be of major importance. Certainly, the role and variations of terminal accessory FimC-E in superstructure formation and/or (co-) adhesion should be investigated in future studies.

In strain OMI 622, which has fimbriae of the particularly apathogenic type V, we were able to detect only a few fimbriae, despite screening hundreds of cells by electron microscopy. These few fimbriae could be due to the reverse mutation of the RE motif into RA, a site responsible for RgpB-protease activation in individual clones (shown in Figures 3 and 4). The rare finding of (single or bundled) fimbriae in OMI 622 as a representative for subtype V could be due to the suboptimal restriction of leader peptide due to this altered restriction site. Evidence for this assumption is that a similar picture of surface structure alternations (almost no fimbriae but more extracellular vesicles) was demonstrated by Tokuda et al. (1996) when Rgp-(1)-activity was eliminated by mutation.

5 | CONCLUSIONS

We amplified the *fimA* and *fimB* genes of 28 selected *P. gingivalis* and six *P. gulae* strains using newly designed primers. We compared/combined results with the 99 publicly available *fimA*/FimA sequences from NCBI's GenBank in an alignment and analyzed clusters and phylogeny based on both *fimA* and FimA. The subtype-specific primers (except those for subtype V) currently used to classify/subtype *fimA* should no longer be used because of too many cross-reactions among genotype and serotypes. A much better approach is to amplify and sequence the entire *fimA* and compare results with references. We could show that at least two new subtypes (IIa, IIb) need to be added to the current classification scheme. Our phylogenetic trees also provide information about the evolution of FimA for the first time. It can be assumed that *P. gingivalis* in humans evolved from animal strains and that there is ongoing cross-host recombination. Among the latter, the particularly apathogenic type V appears to be the youngest in evolutionary terms, being most distant from type I. In addition, we have taken the first close-up electron micrograph of the long (bundled) fimbriae of *P. gingivalis* in strain ATCC 33277 (type I) and could demonstrate fundamental differences in cell-cell inter-knotting and brick-wall-like biofilm formation compared to the most distant type V strain OMI 622, which on the other side shows more intense vesicle production. As we did not investigate Mfa mutants, a contribution of short fimbriae (and

20411014, 2023, 5, Downloaded from https://onlinelibrary.wiley.com/doi/10.1111/omi.12433 by Cochrane Germany, Wiley Online Library on [04/12/2023]. See the Terms and Conditions (https://onlinelibrary.wiley.com/terms-and-conditions) on Wiley Online Library for rules of use; OA articles are governed by the applicable Creative Commons License

other extracellular components such as proteins and vesicles) to superstructure formation can, however, not be excluded or is even likely. The bundling of long fimbriae appears to be a virulence mechanism known from EPEC/EHEC and *Salmonella*, resulting in enhanced surface adhesion and co-aggregation. Overall, our work provides new extensive insights into the diversity, phylogenetic evolution, structure, and function of the long fimbriae of *P. gingivalis*.

AUTHOR CONTRIBUTIONS

Hendrik Leonhard Meyer performed all experiments, collected and analyzed the data, and wrote the manuscript. Mohamed M. H. Abdelbary secured funding, interpreted the data, and corrected the manuscript. Eva Miriam Buhl supervised Hendrik Leonhard Meyer in TEM and SEM experiments, interpreted TEM/SEM data, and corrected the manuscript. Christoph Kuppe contributed to data analysis and corrected the manuscript. Georg Conrads conceived the idea supervised the authors and corrected the manuscript. Hendrik Leonhard Meyer interpreted the data and corrected the manuscript.

ACKNOWLEDGMENTS

The study was supported by the IZKF (Interdisciplinary Center for Clinical Research, grant number OC1-06) of the Medical Faculty, RWTH Aachen, Germany. The Quattro S was funded by the Deutsche Forschungsgemeinschaft (DFG, German Research Foundation, grant number 495328185). We thank Beate Melzer-Krick for her excellent technical assistance.

Open access funding enabled and organized by Projekt DEAL.

CONFLICT OF INTEREST STATEMENT

The authors declare no conflicts of interest.

DATA AVAILABILITY STATEMENT

The data that support the findings of this study will soon be openly available. Gene sequence data are submitted for entry in NCBI/GenBank under accession Nos. OR072649-OR072682.

ORCID

Georg Conrads https://orcid.org/0000-0003-2577-5294

PEER REVIEW

The peer review history for this article is available at https://publons.com/publon/10.1111/omi.12433.

REFERENCES

Abdelbary, M. M. H., Schittenhelm, F., Yekta-Michael, S. S., Reichert, S., Schulz, S., Kasaj, A., Braun, A., Conrads, G., & Stein, J. M. (2022). Impact of three nonsurgical, full-mouth periodontal treatments on total bacterial load and selected pathobionts. *Antibiotics*, *11*(5), 686. https://doi.org/10.3390/antibiotics11050686

Ally, N., Whisstock, J. C., Sieprawska-Lupa, M., Potempa, J., Le Bonniec, B. F., Travis, J., & Pike, R. N. (2003). Characterization of the specificity of arginine-specific gingipains from *Porphyromonas gingivalis* reveals active site differences between different forms of the enzymes. *Biochemistry*, *42*(40), 11693-11700. https://doi.org/10.1021/bi0349726

Alzohairy, A. M. (2011). BioEdit: An important software for molecular biology. *GERF Bulletin of Biosciences*, *2*(1), 60-61.

Amano, A., Nakagawa, I., Kataoka, K., Morisaki, I., & Hamada, S. (1999). Distribution of *Porphyromonas gingivalis* strains with fimA genotypes in periodontitis patients. *Journal of Clinical Microbiology*, *37*(5), 1426-1430. https://doi.org/10.1128/JCM.37.5.1426-1430.1999

Beikler, T., Peters, U., Prajaneh, S., Prior, K., Ehmke, B., & Flemmig, T. F. (2003). Prevalence of *Porphyromonas gingivalis* fimA genotypes in Caucasians. *European Journal of Oral Sciences*, *111*(5), 390-394. https://doi.org/10.1034/j.1600-0722.2003.00065.x

Cai, J., Chen, J., Guo, H., Pan, Y., Zhang, Y., Zhao, W., Li, X., & Li, Y. (2019). Recombinant fimbriae protein of *Porphyromonas gingivalis* induces an inflammatory response via the TLR4/NF-κB signaling pathway in human peripheral blood mononuclear cells. *International Journal of Molecular Medicine*, *43*(3), 1430-1440. https://doi.org/10.3892/ijmm.2019.4069

Chen, M. X., Zhong, Y. J., Dong, Q. Q., Wong, H. M., & Wen, Y. F. (2021). Global, regional, and national burden of severe periodontitis, 1990-2019: An analysis of the Global Burden of Disease Study 2019. *Journal of Clinical Periodontology*, *48*(9), 1165-1188. https://doi.org/10.1111/jcpe.13506

Chen, Q., Shao, Z., Liu, K., Zhou, X., Wang, L., Jiang, E., Luo, T., & Shang, Z. (2021). Salivary *Porphyromonas gingivalis* predicts outcome in oral squamous cell carcinomas: A cohort study. *BMC Oral Health*, *21*(1), 228. https://doi.org/10.1186/s12903-021-01580-6

Coats, S. R., Kantrong, N., To, T. T., Jain, S., Genco, C. A., McLean, J. S., & Darveau, R. P. (2019). The distinct immune-stimulatory capacities of *Porphyromonas gingivalis* strains 381 and ATCC 33277 are determined by the fimB allele and gingipain activity. *Infection and Immunity*, *87*(12). https://doi.org/10.1128/IAI.00319-19

Conrads, G., Barth, S., Mockel, M., Lenz, L., van der Linden, M., & Henne, K. (2017). *Streptococcus tigurinus* is frequent among gtfR-negative *Streptococcus oralis* isolates and in the human oral cavity, but highly virulent strains are uncommon. *Journal of Oral Microbiology*, *9*(1), 1307079. https://doi.org/10.1080/20002297.2017.1307079

Dominy, S. S., Lynch, C., Ermini, F., Benedyk, M., Marczyk, A., Konradi, A., Nguyen, M., Haditsch, U., Raha, D., Griffin, C., Holsinger, L. J., Arastu-Kapur, S., Kaba, S., Lee, A., Ryder, M. I., Potempa, B., Mydel, P., Hellvard, A., Adamowicz, K., . . . Potempa, J. (2019). *Porphyromonas gingivalis* in Alzheimer's disease brains: Evidence for disease causation and treatment with small-molecule inhibitors. *Science Advances*, *5*(1), eaau3333. https://doi.org/10.1126/sciadv.aau3333

Enersen, M., Nakano, K., & Amano, A. (2013). *Porphyromonas gingivalis* fimbriae. *Journal of Oral Microbiology*, *5*, 20265. https://doi.org/10.3402/jom.v5i0.20265

Enersen, M., Olsen, I., Kvalheim, Ø., & Caugant, D. A. (2008). fimA genotypes and multilocus sequence types of *Porphyromonas gingivalis* from patients with periodontitis. *Journal of Clinical Microbiology*, *46*(1), 31-42. https://doi.org/10.1128/JCM.00986-07

Fournier, D., Mouton, C., Lapierre, P., Kato, T., Okuda, K., & Ménard, C. (2001). *Porphyromonas gulae* sp. nov., an anaerobic, gram-negative coccobacillus from the gingival sulcus of various animal hosts. *International Journal of Systematic and Evolutionary Microbiology*, *51*(3), 1179-1189. https://doi.org/10.1099/00207713-51-3-1179

Fujiwara-Takahashi, K., Watanabe, T., Shimogishi, M., Shibasaki, M., Umeda, M., Izumi, Y., & Nakagawa, I. (2020). Phylogenetic diversity in *fim* and *mfa* gene clusters between *Porphyromonas gingivalis* and *Porphyromonas gulae*, as a potential cause of host specificity. *Journal of Oral Microbiology*, *12*(1), 1775333. https://doi.org/10.1080/20002297.2020.1775333

Fujiwara, T., Morishima, S., Takahashi, I., & Hamada, S. (1993). Molecular cloning and sequencing of the fimbrilin gene of *Porphyromonas gingivalis* strains and characterization of recombinant proteins. *Biochemical and Biophysical Research Communications*, *197*(1), 241-247. https://doi.org/10.1006/bbrc.1993.2467

Giltner, C. L., Nguyen, Y., & Burrows, L. L. (2012). Type IV pilin proteins: versatile molecular modules. *Microbiology and Molecular Biology Reviews*, *76*(4), 740-772. https://doi.org/10.1128/MMBR.00035-12

20411014, 2023, 5, Downloaded from https://onlinelibrary.wiley.com/doi/10.1111/omi.12433 by Cochrane Germany, Wiley Online Library on [04/12/2023]. See the Terms and Conditions (https://onlinelibrary.wiley.com/terms-and-conditions) on Wiley Online Library for rules of use; OA articles are governed by the applicable Creative Commons License

Hajishengallis, G., Darveau, R. P., & Curtis, M. A. (2012). The keystone-pathogen hypothesis. *Nature Reviews Microbiology*, *10*(10), 717-725. https://doi.org/10.1038/nrmicro2873

Hamada, S., Amano, A., Kimura, S., Nakagawa, I., Kawabata, S., & Morisaki, I. (1998). The importance of fimbriae in the virulence and ecology of some oral bacteria. *Oral Microbiology and Immunology*, *13*(3), 129-138.

Hasegawa, Y., & Nagano, K. (2021). *Porphyromonas gingivalis* FimA and Mfa1 fimbriae: Current insights on localization, function, biogenesis, and genotype. *Japanese Dental Science Review*, *57*, 190-200. https://doi.org/10.1016/j.jdsr.2021.09.003

Holt, S. C., & Ebersole, J. L. (2005). *Porphyromonas gingivalis*, *Treponema denticola*, and *Tannerella forsythia*: The "red complex", a prototype polybacterial pathogenic consortium in periodontitis. *Periodontology 2000*, *38*, 72-122. https://doi.org/10.1111/j.1600-0757.2005.00113.x

Inaba, H., Nakano, K., Kato, T., Nomura, R., Kawai, S., Kuboniwa, M., Ishihara, K., Ooshima, T., & Amano, A. (2008). Heterogenic virulence and related factors among clinical isolates of *Porphyromonas gingivalis* with type II fimbriae. *Oral Microbiology and Immunology*, *23*(1), 29-35. https://doi.org/10.1111/j.1399-302X.2007.00386.x

Joshi, C., Mezincescu, A., Gunasekara, M., Rudd, A., Botchorichvili, H., Sabir, S., Dospinescu, C., Noman, A., Hogg, D., Cherukara, G., McLernon, D., Hijazi, K., & Dawson, D. (2022). Myocardial infarction risk is increased by periodontal pathobionts: A cross-sectional study. *Scientific Reports*, *12*(1), 18608. https://doi.org/10.1038/s41598-022-19154-z

Kassebaum, N. J., Smith, A. G. C., Bernabé, E., Fleming, T. D., Reynolds, A. E., Vos, T., Murray, C. J. L., Marcenes, W., Abyu, G. Y., Alsharif, U., Asayesh, H., Benzian, H., Dandona, L., Dandona, R., Kasaeian, A., Khader, Y. S., Khang, Y. H., Kokubo, Y., . . . Yonemoto, N. (2017). Global, regional, and national prevalence, incidence, and disability-adjusted life years for oral conditions for 195 countries, 1990-2015: A systematic analysis for the global burden of diseases, injuries, and risk factors. *Journal of Dental Research*, *96*(4), 380-387. https://doi.org/10.1177/0022034517693566

Kebschull, M., Demmer, R. T., & Papapanou, P. N. (2010). "Gum bug, leave my heart alone!"–Epidemiologic and mechanistic evidence linking periodontal infections and atherosclerosis. *Journal of Dental Research*, *89*(9), 879-902. https://doi.org/10.1177/0022034510375281

Lamont, R. J., & Yilmaz, O. (2002). In or out: The invasiveness of oral bacteria. *Periodontology 2000*, *30*, 61-69. https://doi.org/10.1034/j.1600-0757.2002.03006.x

Madianos, P. N., Bobetsis, Y. A., & Offenbacher, S. (2013). Adverse pregnancy outcomes (APOs) and periodontal disease: Pathogenic mechanisms. *Journal of Periodontology*, *84*(Suppl 4), S170-S180. https://doi.org/10.1902/jop.2013.1340015

Maresz, K. J., Hellvard, A., Sroka, A., Adamowicz, K., Bielecka, E., Koziel, J., Gawron, K., Mizgalska, D., Marcinska, K. A., Benedyk, M., Pyrc, K., Quirke, A.-M., Jonsson, R., Alzabin, S., Venables, P. J., Nguyen, K.-A., Mydel, P., & Potempa, J. (2013). *Porphyromonas gingivalis* facilitates the development and progression of destructive arthritis through its unique bacterial peptidylarginine deiminase (PAD). *PLoS Pathogens*, *9*(9), e1003627. https://doi.org/10.1371/journal.ppat.1003627

Martínez, R. E. M., Herrera, J. L. A., Pérez, R. A. D., Mendoza, C. A., & Manrique, S. I. R. (2021). Frequency of *Porphyromonas gingivalis* and fimA genotypes in patients with periodontitis and systemic lupus erythematosus. *Lupus*, *30*(1), 80-85. https://doi.org/10.1177/0961203320969983

Mercado, F., Marshall, R. I., Klestov, A. C., & Bartold, P. M. (2000). Is there a relationship between rheumatoid arthritis and periodontal disease? *Journal of Clinical Periodontology*, *27*(4), 267-272. https://doi.org/10.1034/j.1600-051x.2000.027004267.x

Mihaescu, R., Levy, D., & Pachter, L. (2009). Why neighbor-joining works. *Algorithmica*, *54*(1), 1-24. https://doi.org/10.1007/s00453-007-9116-4

Nagano, K., Hasegawa, Y., Murakami, Y., Nishiyama, S., & Yoshimura, F. (2010). FimB regulates FimA fimbriation in *Porphyromonas gingivalis*. *Journal of Dental Research*, *89*(9), 903-908. https://doi.org/10.1177/0022034510370089

Nakagawa, I., Amano, A., Kimura, R. K., Nakamura, T., Kawabata, S., & Hamada, S. (2000). Distribution and molecular characterization of *Porphyromonas gingivalis* carrying a new type of fimA gene. *Journal of Clinical Microbiology*, *38*(5), 1909-1914. https://doi.org/10.1128/jcm.38.5.1909-1914.2000

Nakagawa, I., Amano, A., Ohara-Nemoto, Y., Endoh, N., Morisaki, I., Kimura, S., Kawabata, S., & Hamada, S. (2002). Identification of a new variant of fimA gene of *Porphyromonas gingivalis* and its distribution in adults and disabled populations with periodontitis. *Journal of Periodontal Research*, *37*(6), 425-432. https://doi.org/10.1034/j.1600-0765.2002.01637.x

Nezu, T., Hosomi, N., Aoki, S., Nishi, H., Nakamori, M., Shiga, Y., Imamura, E., Shintani, T., Kawaguchi, H., & Maruyama, H. (2022). Assessment of serum IgG titers to various periodontal pathogens associated with atrial fibrillation in acute stroke patients. *Journal of Stroke & Cerebrovascular Diseases*, *31*(3), 106301. https://doi.org/10.1016/j.jstrokecerebrovasdis.2021.106301

O'Flynn, C., Deusch, O., Darling, A. E., Eisen, J. A., Wallis, C., Davis, I. J., & Harris, S. J. (2015). Comparative genomics of the genus *Porphyromonas* identifies adaptations for heme synthesis within the prevalent canine oral species *Porphyromonas cangingivalis*. *Genome Biology and Evolution*, *7*(12), 3397-3413. https://doi.org/10.1093/gbe/evv220

Shibata, S., Shoji, M., Okada, K., Matsunami, H., Matthews, M. M., Imada, K., Nakayama, K., & Wolf, M. (2020). Structure of polymerized type V pilin reveals assembly mechanism involving protease-mediated strand exchange. *Nature Microbiology*, *5*(6), 830-837. https://doi.org/10.1038/s41564-020-0705-1

Shimoyama, Y., Ohara-Nemoto, Y., Kimura, M., Nemoto, T. K., Tanaka, M., & Kimura, S. (2017). Dominant prevalence of *Porphyromonas gingivalis* fimA types I and IV in healthy Japanese children. *Journal of Dental Sciences*, *12*(3), 213-219. https://doi.org/10.1016/j.jds.2017.03.006

Sievers, F., & Higgins, D. G. (2021). The clustal omega multiple alignment package. In K. Katoh (Ed.), *Multiple sequence alignment: Methods and protocols* (pp. 3-16). Springer US.

Sohel, I., Puente, J. L., Murray, W. J., Vuopio-Varkila, J., & Schoolnik, G. K. (1993). Cloning and characterization of the bundle-forming pilin gene of enteropathogenic Escherichia coli and its distribution in Salmonella serotypes. *Molecular Microbiology*, *7*(4), 563-575. https://doi.org/10.1111/j.1365-2958.1993.tb01147.x

Stein, J. M., Yekta-Michael, S. S., Schittenhelm, F., Reichert, S., Kupietz, D., Dommisch, H., Kasaj, A., Wied, S., Vela, O., & Stratul, S. I. (2021). Comparison of three full-mouth concepts for the non-surgical treatment of stage III and IV periodontitis: A randomized controlled trial. *Journal of Clinical Periodontology*, *48*(12), 1516-1527. https://doi.org/10.1111/jcpe.13548

Suzuki, Y., Kikuchi, T., Goto, H., Takayanagi, Y., Kawamura, S., Sawada, N., Okabe, T., Suzuki, Y., Kondo, S., Ohno, T., Hayashi, J.-I., & Mitani, A. (2022). *Porphyromonas gingivalis* fimbriae induce osteoclastogenesis via toll-like receptors in RAW264 cells. *International Journal of Molecular Sciences*, *23*(23), 15293. https://doi.org/10.3390/ijms232315293

Tamura, K., Stecher, G., & Kumar, S. (2021). MEGA11: Molecular evolutionary genetics analysis version 11. *Molecular Biology and Evolution*, *38*(7), 3022-3027. https://doi.org/10.1093/molbev/msab120

Tatakis, D. N., & Kumar, P. S. (2005). Etiology and pathogenesis of periodontal diseases. *Dental Clinics of North America*, *49*(3), 491-516. https://doi.org/10.1016/j.cden.2005.03.001

Tokuda, M., Duncan, M., Cho, M. I., & Kuramitsu, H. K. (1996). Role of *Porphyromonas gingivalis* protease activity in colonization of oral surfaces. *Infection and Immunity*, *64*(10), 4067-4073. https://doi.org/10.1128/iai.64.10.4067-4073.1996

Umeda, J. E., Missailidis, C., Longo, P. L., Anzai, D., Wikström, M., & Mayer, M. P. A. (2006). Adhesion and invasion to epithelial cells by fimA genotypes of *Porphyromonas gingivalis*. *Oral Microbiology and Immunology*, *21*(6), 415-419. https://doi.org/10.1111/j.1399-302X.2006.00312.x

Wang, H., Zhang, W., Wang, W., & Zhang, L. (2020). The prevalence of fimA genotypes of *Porphyromonas gingivalis* in patients with chronic periodon-

20411014, 2023, 5, Downloaded from https://onlinelibrary.wiley.com/doi/10.1111/omi.12433 by Cochrane Germany, Wiley Online Library on [04/12/2023]. See the Terms and Conditions (https://onlinelibrary.wiley.com/terms-and-conditions) on Wiley Online Library for rules of use; OA articles are governed by the applicable Creative Commons License

titis: A meta-analysis. *PLoS One*, *15*(10), e0240251. https://doi.org/10.1371/journal.pone.0240251

Wielento, A., Bereta, G. P., Łagosz-Ćwik, K. B., Eick, S., Lamont, R. J., Grabiec, A. M., & Potempa, J. (2022). TLR2 activation by *Porphyromonas gingivalis* requires both PPAD activity and fimbriae. *Frontiers in Immunology*, *13*, 823685. https://doi.org/10.3389/fimmu.2022.823685

Xicohtencatl-Cortes, J., Monteiro-Neto, V., Ledesma, M. A., Jordan, D. M., Francetic, O., Kaper, J. B., & Giron, J. A. (2007). Intestinal adherence associated with type IV pili of enterohemorrhagic Escherichia coli O157:H7. *Journal of Clinical Investigation*, *117*(11), 3519-3529. https://doi.org/10.1172/JCI30727

Xu, Q., Abdubek, P., Astakhova, T., Axelrod, H. L., Bakolitsa, C., Cai, X., Carlton, D., Chen, C., Chiu, H.-J., Chiu, M., Clayton, T., Das, D., Deller, M. C., Duan, L., Ellrott, K., Farr, C. L., Feuerhelm, J., Grant, J. C., Grzechnik, A., . . . Wilson, I. A. (2010). A conserved fold for fimbrial components revealed by the crystal structure of a putative fimbrial assembly protein (BT1062) from *Bacteroides thetaiotaomicron* at 2.2 Å resolution. *Acta Crystallographica Section F*, *66*(10), 1281-1286. https://doi.org/10.1107/S1744309110006548

Yoshimura, F., Murakami, Y., Nishikawa, K., Hasegawa, Y., & Kawaminami, S. (2009). Surface components of *Porphyromonas gingivalis*. *Journal of Periodontal Research*, *44*(1), 1-12. https://doi.org/10.1111/j.1600-0765.2008.01135.x

Zhu, Y., Dashper, S. G., Chen, Y.-Y., Crawford, S., Slakeski, N., & Reynolds, E. C. (2013). *Porphyromonas gingivalis* and *Treponema denticola* synergistic polymicrobial biofilm development. *PLoS One*, *8*(8), e71727. https://doi.org/10.1371/journal.pone.0071727

SUPPORTING INFORMATION

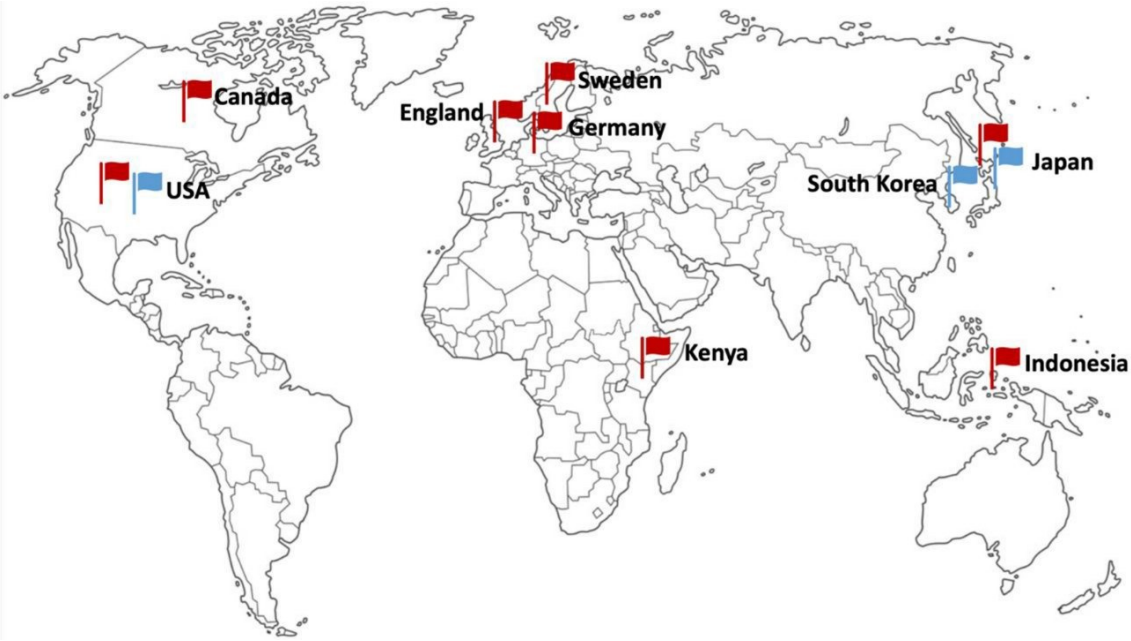
Additional supporting information can be found online in the Supporting Information section at the end of this article.

How to cite this article: Meyer, H. L., Abdelbary, M. M. H., Buhl, E. M., Kuppe, C., & Conrads, G. (2023). Exploring the genetic and functional diversity of *Porphyromonas gingivalis* long fimbriae. *Molecular Oral Microbiology*, *38*, 408-423. https://doi.org/10.1111/omi.12433

20411014, 2023, 5, Downloaded from https://onlinelibrary.wiley.com/doi/10.1111/omi.12433 by Cochrane Germany, Wiley Online Library on [04/12/2023]. See the Terms and Conditions (https://onlinelibrary.wiley.com/terms-and-conditions) on Wiley Online Library for rules of use; OA articles are governed by the applicable Creative Commons License

Supplementary Materials:

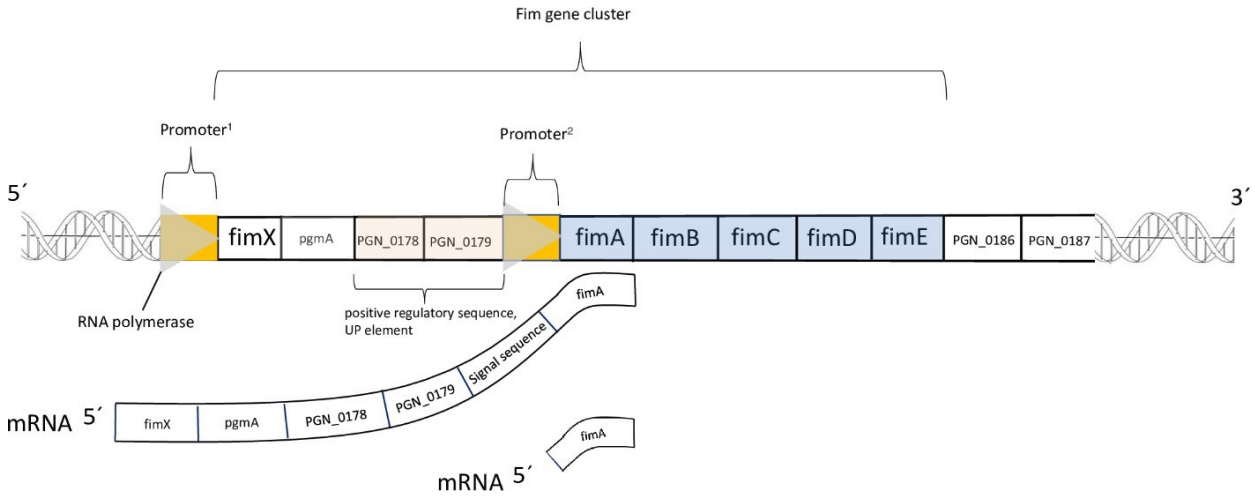
Suppl. Figure 1:



Suppl. Figure 1: Geographical distribution of the 133 *P. gingivalis* strains (isolates and genomes) analyzed in this study.

Red flags: Origin of the isolates from our strain collection, blue flags: Geographical origin of the genomes imported from the GenBank of NCBI (84 from Japan, 11 from USA and 4 from South Korea).

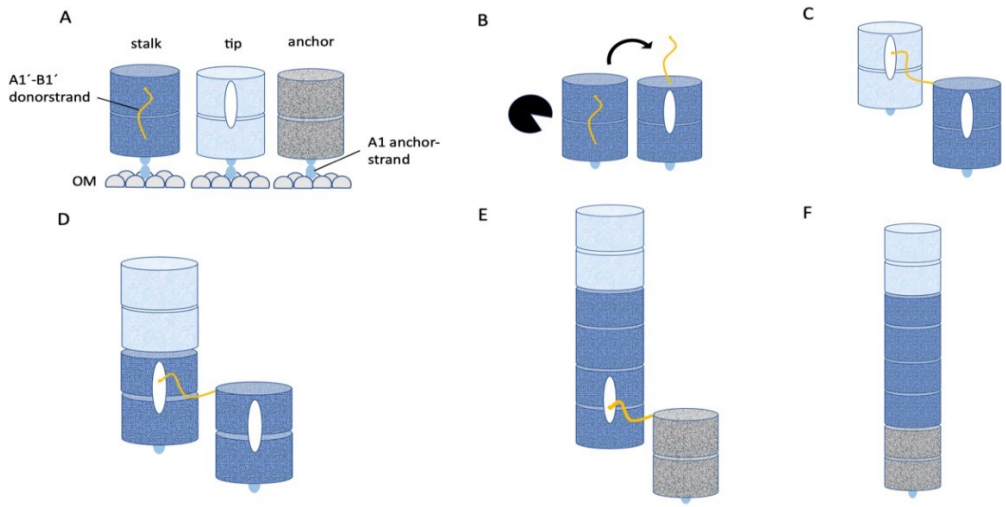
Suppl. Figure 2A:



Suppl. Figure 2A: Genetic map of the *fim*- genes cluster.

The *fim* gene cluster (*fimX, pgmA, fimA, fimB, fimC, fimD*, and *fimE*) encodes for seven proteins with mainly structural function and additional genes for regulation. All genes are present in a single copy and have the same transcription direction. The transcriptional organization of this locus includes a first promoter upstream of *fimX* leading to a polycistronic transcript containing *fimA* (Park et al., 2007) and a second internal promoter located directly upstream of *fimA* (Xie & Lamont, 1999). The activity of the second promoter is increased when additional upstream sequences are present, highlighted in light orange (Xie & Lamont, 1999). Fimbriae contain structural elements encoded by the *fimA* (stalk), *fimB* (anchor), and *fimCDE* (tip) genes (highlighted in blue). The promoters and transcriptional organization of the *fimB* and *fimCDE* genes are currently unknown. Additional regulatory elements are *fimR* and *fimS* (encoded on a different chromosomal section not shown).

Suppl. Figure 2B:

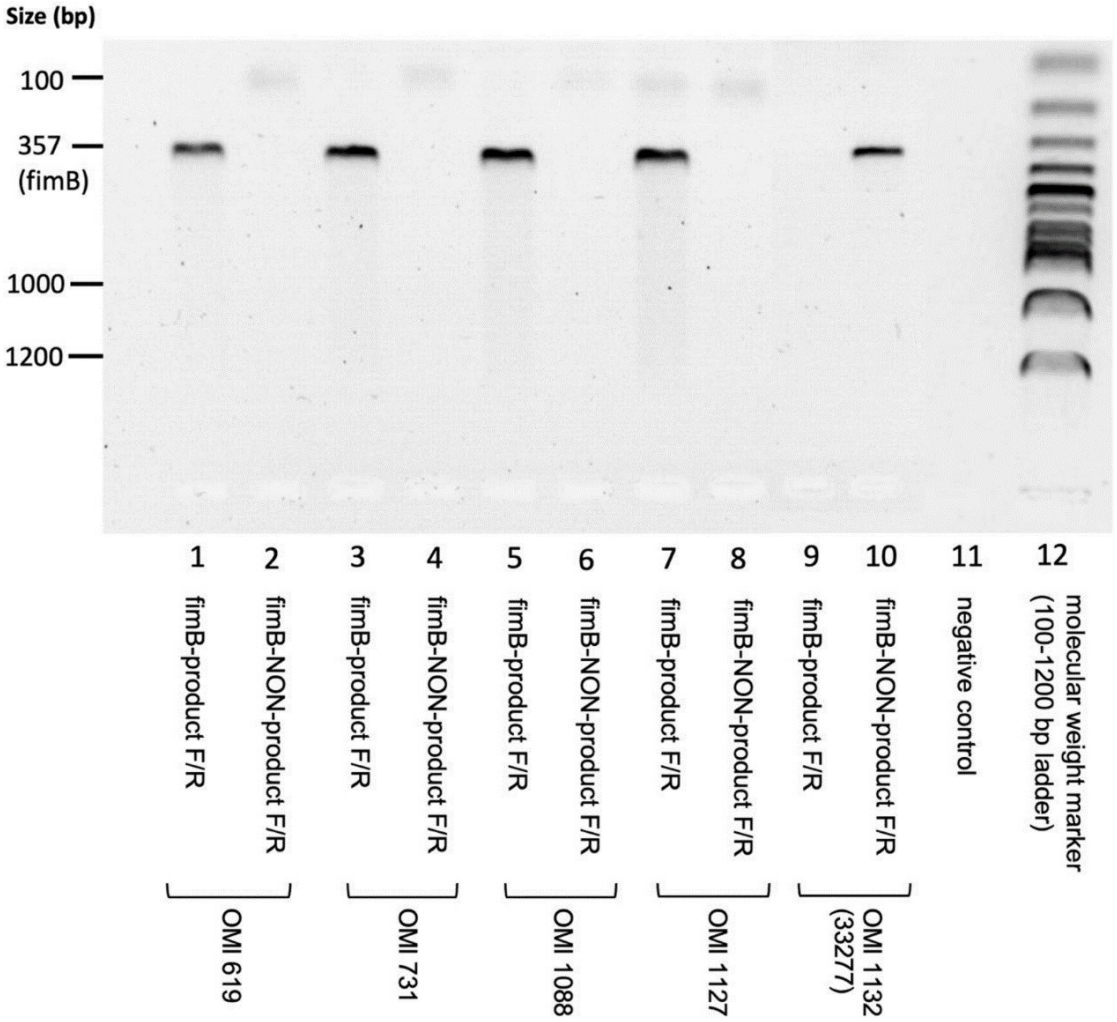


Suppl. Figure 2B: Model for the polymerization of type V fimbriae.

A: There are three types of protein subunits that form the fimbriae and be referred to as the stalk-, tip-, and anchor-protein. All are lipoproteins and lipidated to a conserved cysteine on the outer membrane (OM) of the cell surface. The anchor strand A1 binds the subunit to the outer membrane (OM). Stalk-fimbriae have a protease cleavage site and possess a donor strand (yellow curved line). Tip-fimbriae do not possess a donor strand (indicated by the white ellipse). Anchor-fimbriae do not possess a protease cleavage site. **B**: The enzyme RgpB can bind to the cleavage-site of a stalk-fimbria and activate its initially refolded donor strand. At the same time, a hydrophobic groove ("pocket") is created in the stalk-fimbria (white ellipse). **C**: The activated stalk-fimbria can connect to a tip-fimbria with its donor strand and detach it from the membrane. **D**: Another stalk-fimbria in the same activated state continues polymerization. **E:** The random binding of a non-cleavable anchor-fimbria terminates polymerization because no groove is released to which another fimbria could bind. **F:** Fully polymerized fimbria consisting of a tip-fimbria, several stalk-fimbriae, and a functional anchor-fimbria (the latter not produced by strains ATCC 33277/381).

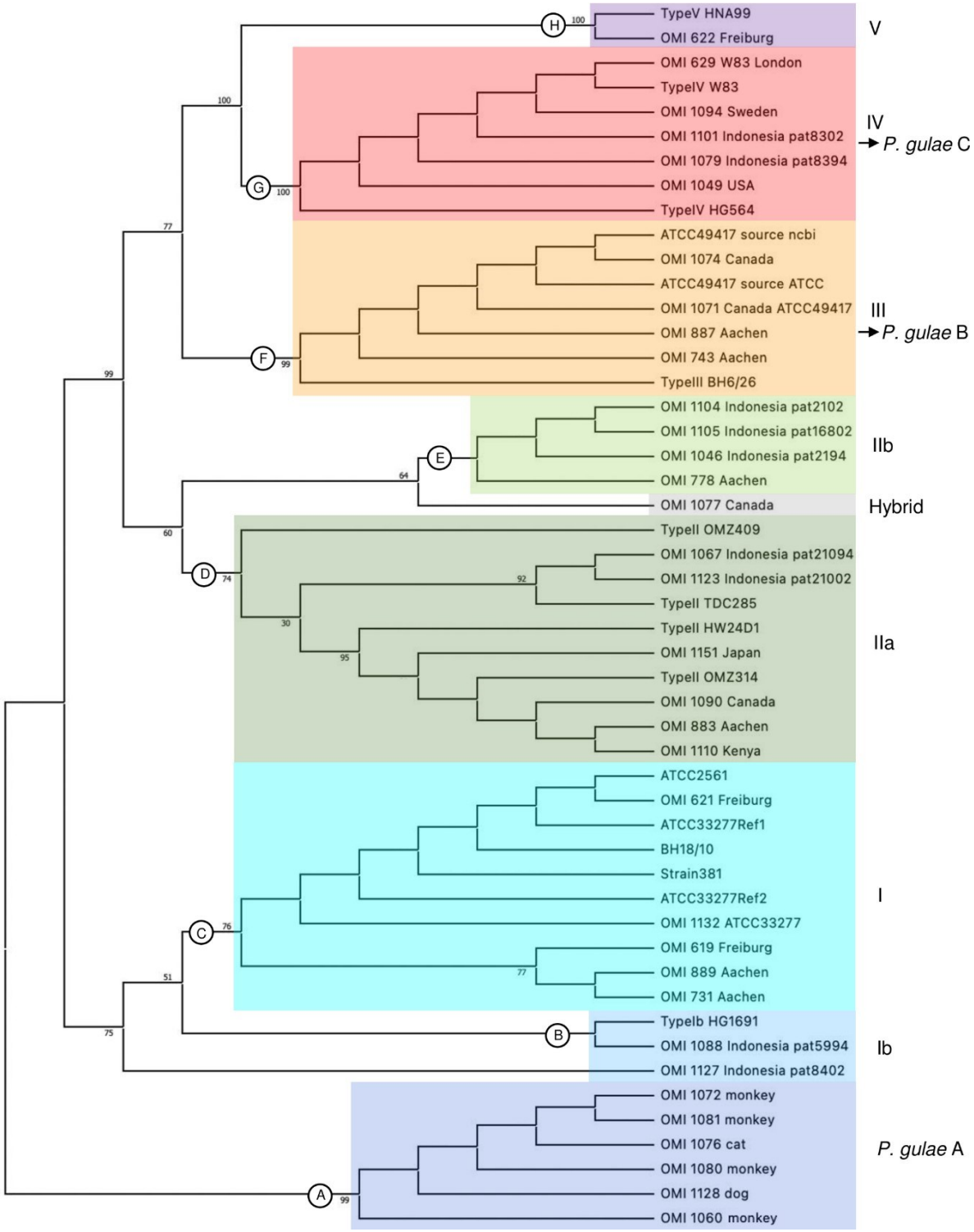
Assembly and function of the FimA protein: background: As nicely investigated and described in the study by Shibata et al. 2020 (Shibata et al., 2020), FimA is synthesized as a preprotein with a signal sequence that enables the translocation of FimA into the periplasm. In the periplasm, signal peptidase II removes the signal sequence and the newly formed N-terminus is lipidated at cysteine of position 19. The lipidated fimbriae are subsequently transported to the outer membrane surface, probably via a lipoprotein sorting machinery. The exact mechanism by which subunits are exported to the cell surface is not yet fully understood, but for the first time studied and described in a publication by Shoji et al. 2020 (Shoji et al., 2020). In the same study, the crystal structure of the FimA monomer was also elucidated. Fimbriae are structurally conserved and have distinct N-terminal (NTD) and C-terminal domains (CTD). Each domain has a transthyretin-like fold and consists of seven β-strands arranged in two β-sheets (Shibata et al., 2020). Furthermore, it has been found that the fimbriae of P. gingivalis undergo a unique assembly called "donor-strand exchange" that occurs in a similar manner in the type I fimbriae of E.coli (Nishiyama et al., 2008). The mechanism of polymerization is shown in Suppl. Figure 2B above..

Suppl. Figure 2C:



Supplementary Figure 2C: Switch-PCR for Stop codon detection within *fimB*. Results of five isolates, of which four could be amplified with the primer pair fimB-product F/R (lane 1, 3, 5 and 7) but not with the primer pair fimB-NON-product F/R (lane 2, 4, 6, and 8) (y/n). In contrast to all others, strain ATCC 33277 could not be amplified with the primer pair fimB-product F/R (lane 9) but with fimB-NON-product F/R (lane 10) (n/y). Isolates are ordered from left to right in lanes: 1, 2: OMI 619; 3, 4: OMI 731; 5, 6: OMI 1088; 7, 8: OMI 1127; 9,10: OMI 1132 (ATCC 33277); 11: negative control, 12: molecular weight marker.

Suppl. Figure 3A



Suppl. Figure 3A: Phylogenetic tree (cladogram) based on *fimA* genotypes (**without** leader signal sequence) of 50 *P. gingivalis* strains.

Suppl. Figure 3B



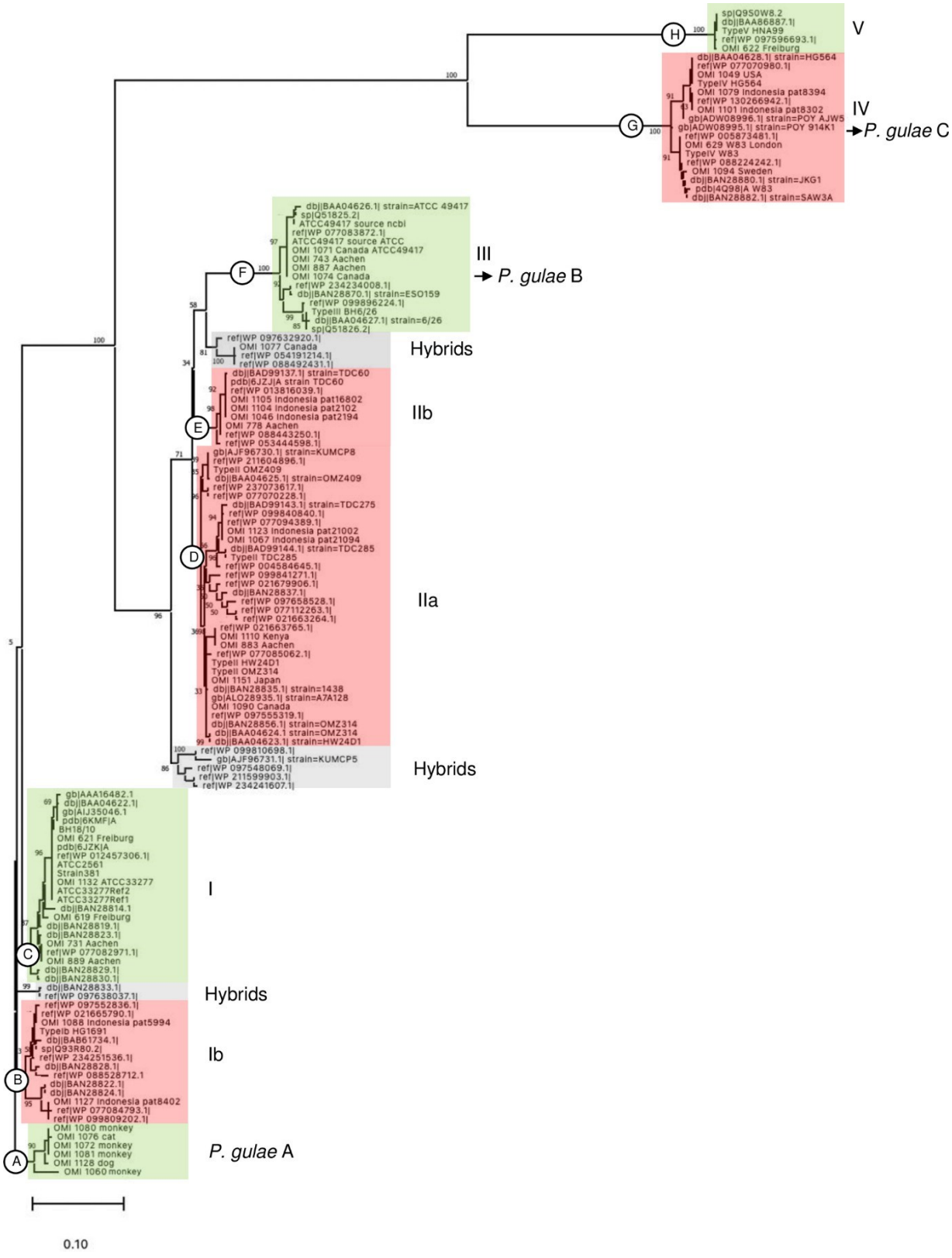
Suppl. Figure 3B: Phylogenetic tree (phylograms) based on *fimA* genotypes (**without** leader signal sequence) of 50 *P. gingivalis* strains. Green: strains generally associated with periodontal health, red: strains generally associated with periodontal disease, grey: hybrid strain.

Suppl. Figure 3C



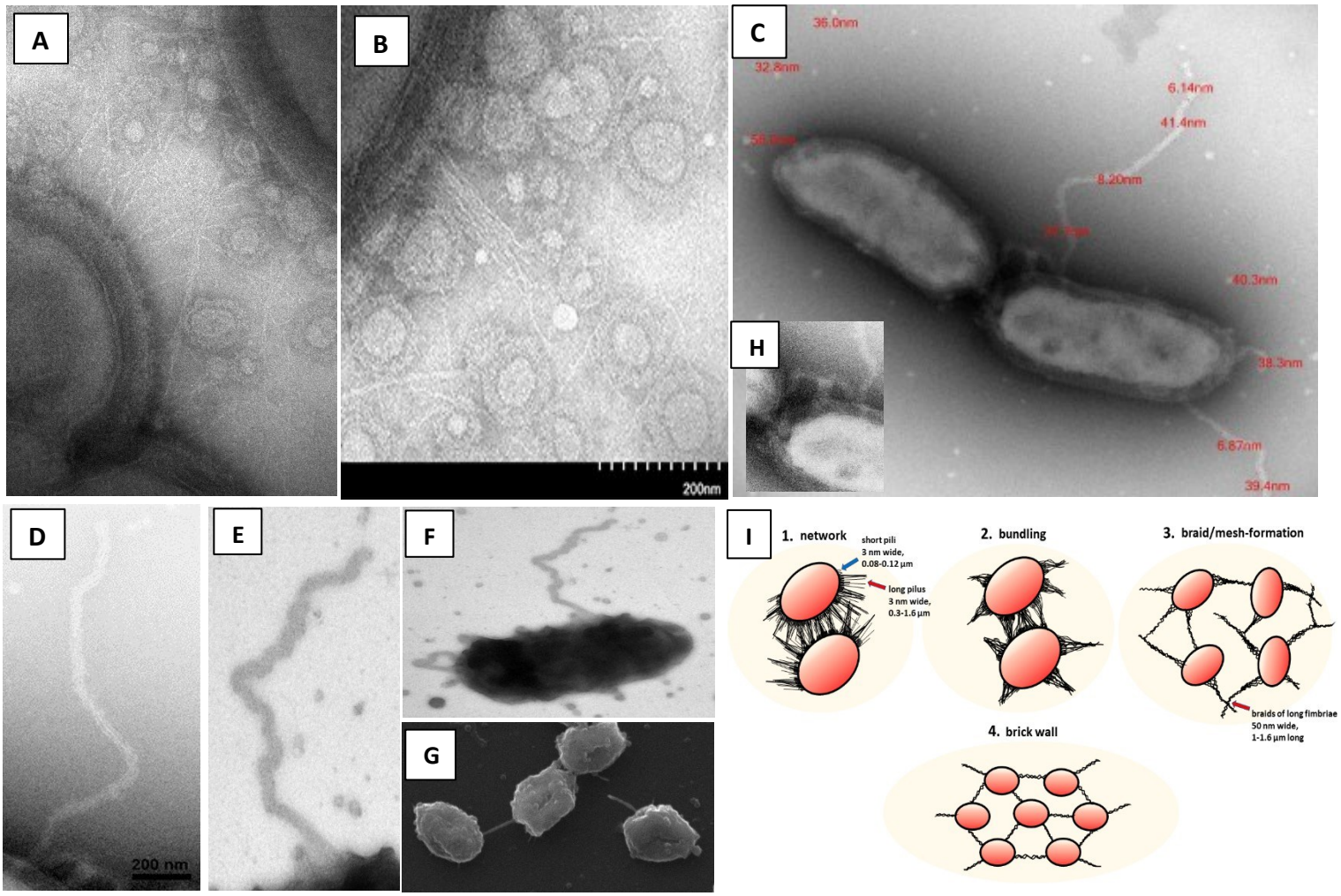
Supplementary Figure 3C: Phylogenetic tree (cladogram) based on FimA serotypes (**without** signal sequence) of 133 *P. gingivalis* strains. Be aware that in this particular calculation subtype IIb is even closer related to subtype III than to subtype IIa, which pronounces the need for separation. All other calculations, especially those of phylograms, proof the IIa/b relatedness.

Suppl. Figure 3D



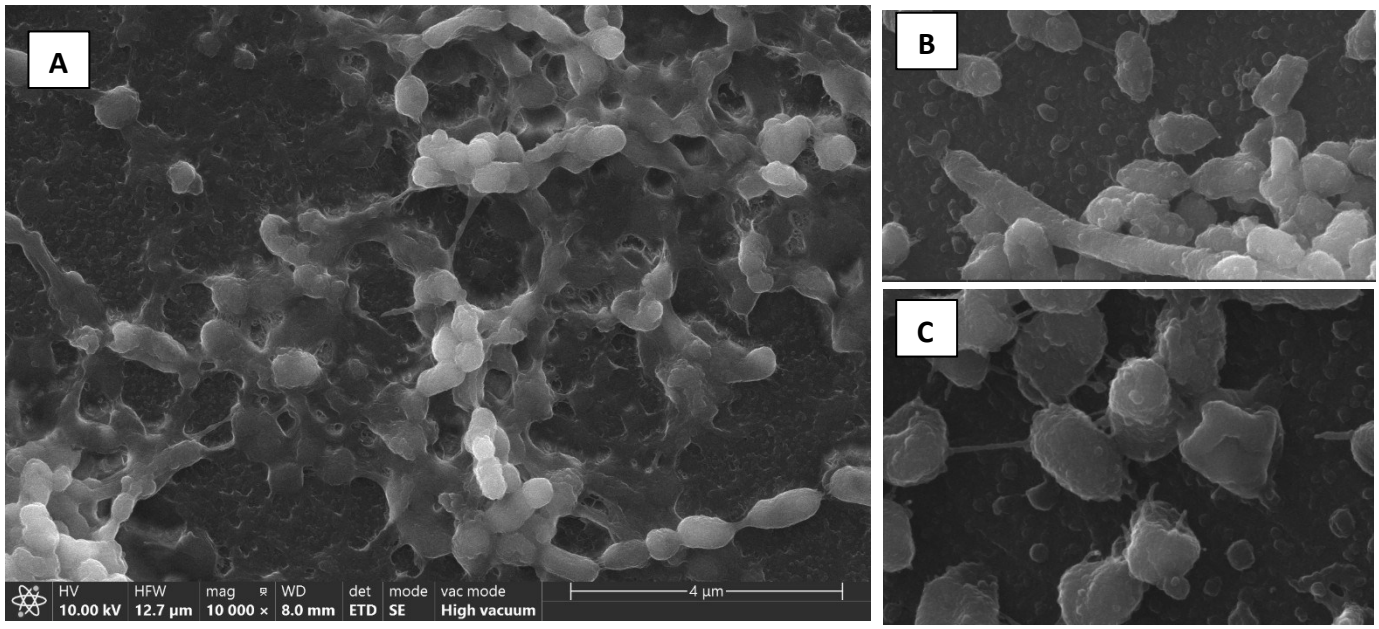
Supplementary Figure 3D: Phylogenetic tree (phylogram) based on FimA serotypes (**without** signal sequence) of 133 *P. gingivalis* strains. Green: strains generally associated with periodontal health, red: strains generally associated with periodontal disease, grey: hybrids.

Suppl. Figure 4A:



Supplementary Figure 4A: Long fimbriae of *P. gingivalis* ATCC 33277 (subtype I fimbriae, >130 nm) forming (**A)** net-work structures, and (**B)** a few might occasionally bundle. If bundling (matting) continues, a few bundles form braid-like super-structures (compare with Tokuda et al., 1996[Fig. 5] or Chandad and Mouton 1995, the latter applying immunolabelling [Figs. 6 and 7]). The braid- or mesh-like super-structures are between 30 and 50 nm wide (**C**), up to 1,500 nm long (**D** [detail of C) **+ E** [detail of F]), are robust and withstand harsh preparation conditions, such as in TEM after a centrifugation step **(C- F**), or as in REM-preparation **(G)**, and might knot cells together (**H,** detail of C), finally even forming a brick wall biofilm (compare with Zhu et al. 2013 [Figure 5b]). **I)** Four steps of *P. gingivalis* fimbriae braid-, mesh- and brick-wall- formation. Compare with images of bundled pili of EPEC/EHEC (Xicohtencatl-Cortes et al., 2007).

Suppl. Figure 4B:



Supplementary Figure 4B: *P. gingivalis* OMI 622 (type V fimbriae) forming **A)** slimy net-work structures, **B)** a few, elongated and filamentous cells, and **C)** very rarely bundled fimbriae. The rare finding of (single or bundled) fimbriae could be due to suboptimal restriction of leader peptide due to altered restriction site as a similar picture was demonstrated by Tokuda et al. 1996, when Arg-gingipain activity was eliminated by mutation.

REFERENCES

Chandad, F., & Mouton, C. (1995). Antigenic, structural, and functional relationships between fimbriae and the hemagglutinating adhesin HA-Ag2 of *Porphyromonas gingivalis*. *Infection and Immunity, 63*(12), 4755-4763. doi:doi:10.1128/iai.63.12.4755-4763.1995

Nishiyama, M., Ishikawa, T., Rechsteiner, H., & Glockshuber, R. (2008). Reconstitution of Pilus Assembly Reveals a Bacterial Outer Membrane Catalyst. *Science, 320*(5874), 376-379. doi:doi:10.1126/science.1154994

Park, Y., Xie, H., & Lamont, R. J. (2007). Transcriptional organization of the *Porphyromonas gingivalis fimA* locus. *FEMS Microbiol Lett, 273*(1), 103-108. doi:10.1111/j.1574-6968.2007.00782.x

Shibata, S., Shoji, M., Okada, K., Matsunami, H., Matthews, M. M., Imada, K., . . . Wolf, M. (2020). Structure of polymerized type V pilin reveals assembly mechanism involving protease-mediated strand exchange. *Nature Microbiology, 5*(6), 830-837. doi:10.1038/s41564-020-0705-1

Shoji, M., Shibata, S., Sueyoshi, T., Naito, M., & Nakayama, K. (2020). Biogenesis of Type V pili. *Microbiol Immunol, 64*(10), 643-656. doi:10.1111/1348-0421.12838

Tokuda, M., Duncan, M., Cho, M. I., & Kuramitsu, H. K. (1996). Role of *Porphyromonas gingivalis* protease activity in colonization of oral surfaces. *Infection and Immunity, 64*(10), 4067-4073. doi:doi:10.1128/iai.64.10.4067-4073.1996

Xicohtencatl-Cortes, J., Monteiro-Neto, V., Ledesma, M. A., Jordan, D. M., Francetic, O., Kaper, J. B., . . . Giron, J. A. (2007). Intestinal adherence associated with type IV pili of enterohemorrhagic Escherichia coli O157:H7. *J Clin Invest, 117*(11), 3519-3529. doi:10.1172/JCI30727

Xie, H., & Lamont, R. J. (1999). Promoter architecture of the *Porphyromonas gingivalis* fimbrillin gene. *Infection and Immunity, 67*(7), 3227-3235. doi:doi:10.1128/iai.67.7.3227-3235.1999

Zhu, Y., Dashper, S. G., Chen, Y.-Y., Crawford, S., Slakeski, N., & Reynolds, E. C. (2013). *Porphyromonas gingivalis* and *Treponema denticola* Synergistic Polymicrobial Biofilm Development. *PLOS ONE, 8*(8), e71727. doi:10.1371/journal.pone.0071727

Erklärung § 5 Abs. 1 zur Datenaufbewahrung

Hiermit erkläre ich, dass die dieser Dissertation zu Grunde liegenden Originaldaten

bei mir, Hendrik Leonhard Meyer, Alte Dorfstraße 48, 22397 Hamburg

hinterlegt sind.

Erklärung gemäß § 5 Abs. (1) und (2), und § 11 Abs. (3) 12. der Promotionsordnung[1]

Hiermit erkläre ich, **Hendrik Leonhard Meyer,** an Eides statt, dass ich den wesentlichen Anteil an der Publikation:[1]
Doktorand Hendrik Leonhard Meyer., Prakt. Betreuer Dr. rer. nat. Mohamed M. H. Abdelbary, Projektplanung TEM & REM Dr. rer. nat. Eva Miriam Buhl, Oberarzt Priv. Doz. Dr. med. Christoph Kuppe, Doktorvater Univ.-Prof. Dr. rer. nat. Georg Conrads**.:**

[Exploring the genetic and functional diversity of Porphyromonas gingivalis long fimbriae]; [Molecular Oral Microbiology].; first published 26 September 2023, geleistet habe.

Die Anteile an der Arbeit waren wie folgt:

Bitte Namen angeben ----------->	Doktorand / Hendrik Leonhard Meyer	Prakt. Betreuer / Dr. rer. nat. Mohamed M. H. Abdelbary	Projekt-planung TEM & REM / Dr. rer. nat. Eva Miriam Buhl	Oberarzt / Priv. Doz. Dr. med. Christoph Kuppe	Doktorvater / Univ.-Prof. Dr. rer. nat. Georg Conrads	Summe (%)
Studienüberwachung		30			70	100
Studiendesign/Konzeption	20	10			70	100
Datenauswertung	**100**					100
Durchführung der Experimente	**100**					100
Bereitstellung von Materialien			5		95	100
Interpretation der Datenauswertung	40	10	10	5	35	100
Verfassung des Manuskripts	**100**					100
Korrektur des Manuskripts	30	5	5	5	55	100

Aus diesem wesentlichen Anteil ergibt sich selbstverständlich die Stellung als Erstautor / in.

_____
Unterschrift der Doktorandin/des Doktoranden

Als Doktorvater und korrespondierender Autor bestätige ich die Angaben von Herrn Hendrik Leonhard Meyer.

_____ _____
Unterschrift des Doktorvaters Unterschrift des korresp. Autors (falls abweichend)

Erklärung gemäß § 5 Abs. (1) und (2), und § 11 Abs. (3) 12. der Promotionsordnung[4]

Hiermit erkläre ich, **Hendrik Leonhard Meyer,** an Eides statt, dass ich den wesentlichen Anteil an der Publikation:[1]
Doktorand Hendrik Leonhard Meyer., Prakt. Betreuer Dr. rer. nat. Mohamed M. H. Abdelbary, Projektplanung TEM & REM Dr. rer. nat. Eva Miriam Buhl, Oberarzt Priv. Doz. Dr. med. Christoph Kuppe, Doktorvater Univ.-Prof. Dr. rer. nat. Georg Conrads**.:**

[Exploring the genetic and functional diversity of Porphyromonas gingivalis long fimbriae]; [Molecular Oral Microbiology].; first published 26 September 2023, geleistet habe.

Die Anteile an der Arbeit waren wie folgt:

Bitte Namen angeben ----------->	Doktorand / Hendrik Leonhard Meyer	Prakt. Betreuer / Dr. rer. nat. Mohamed M. H. Abdelbary	Projekt-planung TEM & REM / Dr. rer. nat. Eva Miriam Buhl	Oberarzt / Priv. Doz. Dr. med. Christoph Kuppe	Doktorvater / Univ.-Prof. Dr. rer. nat. Georg Conrads	Summe (%)
Studienüberwachung		30			70	100
Studiendesign/Konzeption	20	10			70	100
Datenauswertung	**100**					100
Durchführung der Experimente	**100**					100
Bereitstellung von Materialien			5		95	100
Interpretation der Datenauswertung	40	10	10	5	35	100
Verfassung des Manuskripts	**100**					100
Korrektur des Manuskripts	30	5	5	5	55	100

Ich schließe mich der Erklärung von Herrn Univ.-Prof. Dr. rer. nat. Georg Conrads als Koautor an.

_____
Dr. rer. nat. Mohamed M. H. Abdelbary

_____
Dr. rer. nat. Eva Miriam Buhl

_____
Priv. Doz. Dr. med. Christoph Kuppe